

CHALMERS



High Speed Braking Stability

Master's thesis in Applied Mechanics

BJÖRN ANDERSSON
PATRIC GILLBERG

Department of Applied Mechanics
Division of Dynamics
CHALMERS UNIVERSITY OF TECHNOLOGY
Göteborg, Sweden 2013
Master's thesis 2013:53

MASTER'S THESIS IN APPLIED MECHANICS

High Speed Braking Stability

BJÖRN ANDERSSON
PATRIC GILLBERG

Department of Applied Mechanics
Division of Dynamics
CHALMERS UNIVERSITY OF TECHNOLOGY
Göteborg, Sweden 2013

High Speed Braking Stability
BJÖRN ANDERSSON
PATRIC GILLBERG

© BJÖRN ANDERSSON, PATRIC GILLBERG, 2013

Master's thesis 2013:53
ISSN 1652-8557
Department of Applied Mechanics
Division of Dynamics
Chalmers University of Technology
SE-412 96 Göteborg
Sweden
Telephone: +46 (0)31-772 1000

Cover:

A NASCAR driver spins out after an accident in a race in the NASCAR Sprint Cup Series Ford 400 at Homestead-Miami Speedway on November 20, 2011 in Homestead, Florida. Source:

http://www.zimbio.com/photos/Jimmie+Johnson/Ford+400/W-8ezrWjZj_

Chalmers Reproservice
Göteborg, Sweden 2013

High Speed Braking Stability
Master's thesis in Applied Mechanics
BJÖRN ANDERSSON
PATRIC GILLBERG
Department of Applied Mechanics
Division of Dynamics
Chalmers University of Technology

ABSTRACT

A key factor, if not *the* key factor, when operating a road vehicle safely is the stability when controlling the vehicle's motion. The stability during cornering at moderate lateral accelerations has to a large extent been studied and the vehicle behaviour and theory for these manoeuvres are well documented. The stability of a vehicle performing hard braking at high speed has however not yet been studied to the same extent and a complete theory for these manoeuvres is so far undefined. The derivation of such a theory is of significance since a vehicle travelling at high speed is sensitive to external disturbances and to steering inputs from the driver.

The thesis is to a large extent based on the article *Skidding of vehicles due to locked wheels*, by Professor Warner T. Koiter and Professor Hans B. Pacejka, where an analytical expression for the yaw velocity for a simple vehicle model is derived and studied. In this thesis that model is confirmed and developed even further by adding additional effects to the model and by achieving better analytical solvability. Further studies regarding the impact and importance of how different vehicle dynamical effects influence the possibility to obtain a closed form solution and output in terms of lateral drift and yaw velocity are also performed.

The main output of the thesis is an analytical model of a flat two wheel vehicle, from which it is possible to obtain analytical expressions for the yaw velocity, lateral drift and lateral acceleration during high speed braking with a small disturbance to the system. The disturbance analysed is mainly a constant yaw moment, however the model is also capable of including a constant lateral force. Physical interpretations of the disturbances can be seen as an uneven brake distribution or a constant side wind. The thesis also presents a study on how different effects, such as lateral force steer and combined slip, influence the vehicle motion and stability outputs.

The subject studied in the thesis is of great importance as a vehicle travelling at high speed easily becomes unstable. The main outputs of the thesis satisfies the research question posed, if not completely then to a large extent. The analytical model shows potential for further development since only one of the vehicle dynamic effects studied in the thesis have been included in the analytical model. The analytical vehicle model is therefore far from fully developed. The quality of the model is so far undetermined as the crucial step of comparing the model against experimental data is yet to be done.

Keywords: Vehicle dynamics, vehicle handling, hard braking, high speed, yaw velocity, lateral drift, analytical vehicle model

ACKNOWLEDGEMENTS

We would like to acknowledge and share the credit of this thesis work with our mentor Mathias Lidberg and our examiner Peter Folkow who have been a big help and motivation throughout the thesis work. We would also like to thank them both for giving us the opportunity to work with this project. Finally we thank Anders Boström and the people working at the Vehicle Dynamics and the Dynamics departments of the Applied Mechanics institution at Chalmers for their helpfulness.

NOMENCLATURE

α_i	Slip angle on axle i
$\bar{\mathcal{L}}$	The Lagrangian expressed with quasi-coordinates
\bar{T}	The kinetic energy expressed only with quasi-coordinates
Ω	Rotational velocity
I	Moment of inertia
m	Mass matrix
r_{pos}	Position vector for the body's center of mass, expressed in the xyz coordinate system
v_{xyz}	Velocity of the origin of the xyz coordinate system
v_{CoM}	Velocity of the body's center of mass
$\Delta F_{z,i,lift}$	Aerodynamic lift force
δ	Steer angle
δ_D	The Dirac delta function
ΔK_{ij}	The spring compression on the i :th axle, on the j :th side
δ_{sp}	Kronecker's delta
δ_{Ts}	Steer angle due to lateral forces
l	Length of the vehicle
l_{dist}	Distance from CoM to the point of attack for the disturbance force
η	Pitch angle
γ_{bd}	Brake distribution front rear
\mathcal{L}	The Lagrangian
μ	Friction coefficient
ω	Eigenfrequency
ω_s	Quasi-coordinates
ω_{lim}	Limit for allowed eigenfrequency
Ψ	Yaw angle
ρ	Air density
ε	Understeer gradient
φ	roll angle
ξ	Damping coefficient
ξ_{Tr}	Pneumatic trail
A	Frontal area
a	Distance from the CoM to the front axle
a_x	Longitudinal acceleration
a_y	Lateral acceleration
B	Tyre stiffness factor
b	Distance from the CoM to the rear axle
C	Shape factor
C_L	Lift force coefficient
$C_{F\alpha i}$	Cornering stiffness for axle i

$C_{F\alpha i}^*$	Equivalent cornering stiffness
CoM	Centre of Mass
D	Peak value of the tyre force
D_f	Cornering compliance for the front axle
d_f	Cornering compliance for the front axle normalized with the gravity constant
D_r	Cornering compliance for the rear axle
d_r	Cornering compliance for the rear axle normalized with the gravity constant
E	Curve factor
F_{avr}	Average static normal force
F_{dist}	Disturbance force
F_{xi}	Longitudinal force/braking force acting on axle i
F_{yi}	Lateral force acting on axle i
F_{zi}	Normal force acting on axle i
g	Gravity constant
h	Distance from the ground plane to the CoM
K_y	Lateral stiffness of the tyres
$k_{i\varphi}$	Torsional stiffness for the i :th axle
K_{ij}	Spring coefficients for the suspension on the i :th axle, on the j :th side
m	Mass of the vehicle
M_{yaw}	Disturbance (yaw) moment
P_{dist}	Magnitude of the disturbance force
Q_i	Generalized forces
q_k	Generalized coordinates
R	Turning radius
r_{lim}	Limit for allowed yaw velocity
T	Kinetic energy
T_s	Torque steer
V	Potential energy
w	Width of the vehicle
Y_{lim}	Limit for allowed lateral drift

CONTENTS

1 Introduction	1
1.1 Background	1
1.2 Problem statement	2
1.3 Purpose	2
1.4 Limitations	2
1.5 Software	3
1.6 Key results	3
1.7 Report outline	3
2 Theory	4
2.1 Vehicle dynamics terminology	4
2.1.1 Vehicle motion	4
2.1.2 Tyre model	5
2.1.3 Steering effects	6
2.1.4 Aerodynamic lift effects	8
2.1.5 Quasi steady state vehicle motion	8
2.2 Lagrange equation for quasi-coordinates	8
2.3 Differential equations	10
2.3.1 Differential equation classification	10
2.3.2 Linearization of differential equation	11
2.3.3 State space representation	12
2.3.4 Ordinary differential equation	12
2.3.4.1 Homogeneous solution, constant coefficients	12
2.3.4.2 Homogeneous solution, variable coefficients	13
2.3.4.3 Particular differential equation solution	13
2.4 Stability definition	13
3 General equations of motion for a vehicle	15
3.1 Derivation of motion equations for a basic four wheel model	15
3.2 From a four wheel model to a two wheel model	19
3.3 Derivation of the differential equation for the yaw velocity	20
3.3.1 Constitutive relations for the tyre slip angles	20
3.3.2 Linearisation of motion equations	21
3.3.3 Operating point of interest	21
3.3.4 Reduction to a single differential equation	21
4 Combining two solution approaches to obtain the two wheel model	23
4.1 Vehicle parameters	23
4.2 Combining Bessel- and constant velocity solutions yields the two wheel model	23
4.2.1 Time dependant coefficients in the differential equation	23
4.2.2 Constants coefficients in the differential equation	25
4.2.3 Analytical solution to the two wheel model	26
4.2.4 Derivation of initial conditions	26
4.2.5 Comparing results of differential equation solution procedures	27
4.3 Validation of the two wheel model	28
4.3.1 Solving the equations of motion for the four wheel model	28
4.3.2 Comparison of the two and four wheel model	29

5	Model analysis	31
5.1	Frequency analysis	31
5.1.1	Eigenfrequency	31
5.1.2	Frequency response	32
5.2	Stability analysis	34
5.2.1	Multiple limits of stability, safety, and comfortability	34
5.2.2	Compromise of the desirable characteristics	36
5.3	Effects of additional model refinements	38
6	Discussion	42
6.1	Compilation of obtained results	42
6.2	Influence of assumptions and limitations	43
6.3	Future recommendations	44
7	Conclusion	45

1 Introduction

When operating a road vehicle the stability of motion is the key factor for safe driver operation. The stability during cornering at moderate lateral accelerations has been studied to a large extent and the theories for these manoeuvres are well established. For straight line braking at moderate speed and braking input the situation is the same, the theory is quite well known. However, severe straight braking manoeuvres at high speed has not yet been studied to the same extent. As a result of this, the major contributing factors to vehicle stability at these kind of operating conditions and manoeuvres are not fully known.

1.1 Background

As the usage of road vehicles are growing and branching out worldwide so is the need for technical development of the subject. From 1970 to 2005 the number of registered vehicles in the world has grown from 246 million vehicles to over 800 million and the number of produced vehicles from 30 million to 65 million per year [16]. This clearly shows the growth of the industry which in turn motivates and accentuates the need of continued research within the field to ensure future progress and expansion of this specific branch of knowledge.

During the 19th and 20th century great advances and achievements were made in the field of complex dynamic mechanical systems which gave birth to numerous methods of describing and deriving equations of motion, all with their own advantages and disadvantages [4]. As road vehicles are highly dynamical systems the utilisation of the governing motion equations has come be of great importance in the process to ensure that the vehicle characteristics are as safe as possible. The immense progress in computational power of computers in the second half of the 20th century, and today still, has lead to that the size, complexity, and reliability in simulations of dynamic mechanical systems has increased continuously. This has given rise to many changes in the approach of developing road vehicles, many of these in the direction of safety and performance [18].

Even though the advances within the field of vehicle dynamics have been many, and the progress continues, modelling of dynamic vehicle behaviour is still very challenging. The broad spread in operating conditions, such as road properties, vehicle characteristics, and speed of travel, complicates the derivation of general theories which leads an equally broad spread in research focusing on different subtopics [9]. One fundamental branch of the vehicle dynamics research that historically has been difficult to deal with, and still is today, is tyre dynamics. It is fundamental in the sense that all environmental interaction (all except air-resistance and gravitational induced interactions) of the vehicle is done through the tyres. In 1956 Professor George Temple wrote

”The complexity of the structure and behaviour of the tire are such that no complete and satisfactory theory has yet been propounded. The characteristics of the tire still presents a challenge to the natural philosopher to devise a theory which shall coordinate the vast mass of empirical data and give some guidance to the manufacturer and user. This is an inviting field for the application of mathematics to the physical world”

regarding tyre shimmy, which according to vehicle dynamics expert Professor Hans B. Pacejka to a large extent still holds true [15]. Although the knowledge regarding tyre dynamics has grown significantly there are still aspects of the field tyre behaviour that are hard to describe mathematically. One of these areas is hard braking at high speed, which with safety being a key factor in the vehicle industry is an important area of research not to be overlooked. Despite that the speed of travel considered here may be well above everyday usage, the fact stands that stable braking, deceleration at any possible magnitude, is a key factor, if not *the* key factor, for safe driver operation of the vehicle.

1.2 Problem statement

The thesis studies the stability of a vehicle in the case of high speed, straight line braking with small disturbances to the system. The disturbances considered in the thesis are constant yaw moment and constant lateral force. The work of the thesis consists of two parts:

- Derive an analytical vehicle model that captures the dynamic behavior of a vehicle during sudden braking with small a disturbance at high speed and validate this analytical model by comparison with an more advanced numerical vehicle model
- Analyse the stability of the analytical model and study which, and how vehicle dynamic related effects influence the out come of the analysis

Thereby the thesis will deliver two separate but still strongly connected outputs. The main focus of the thesis will be on deriving an analytical vehicle model with the aim of taking the research of analytical vehicle models one step further than the present day analytical models.

1.3 Purpose

The purpose of this research is to evaluate if the mathematical models currently used to describe the vehicle dynamics is sufficiently accurate for a stability analysis during high speed braking, or if there is a need for a better mathematical model and what the benefits of a more accurate model would be. This is to be determined by taking the study through the following steps of the project:

- Derivation of a rudimentary analytical vehicle model, both time-variant and invariant
- System stability analysis
- Simulation of a complete model to verify the assumptions made

By carrying out these steps the scientific enquiry posed in Section 1.2 will be answered.

1.4 Limitations

For the thesis work to be feasible and be able to obtain usable results, the scope of the thesis will be governed by the following limitations and simplifications:

- No experimental data to validate the analytical model
- Focus on small deviations from an operating point
- Consistent tyre and suspension characteristics for all speeds and braking conditions
- The roll- and pitch-axis are assumed to be located at the ground plane
- The vehicle is assumed to be rigid
- Disturbances from uneven road surfaces are neglected
- No driver model giving steering wheel input is used

Factors omitted by the limitations are, whilst being important factors for vehicle dynamics, considered to be well known areas of research and therefore not to be considered in the thesis work. These entrained simplifications will isolate the factors governing vehicle stability relevant for the research.

1.5 Software

The thesis is to a large extent carried out with pen and paper since derivation of analytical expressions, free-body-diagrams, and suchlike are significant parts of the study. However, the hand calculations are greatly assisted by computer softwares which also are used to solve the derived expressions. This is carried out by use of the following software programs:

- Matlab 2012b
- Wolfram Mathematica 8.04

An important note for the interested reader is that the Matlab program files written during the thesis work require the version stated above, or a later version. This is due to the updates in the Matlab Symbolic Math Toolbox, which is frequently used in the study. Wolfram Mathematica is used as much as possible, to verify the analytic results of the Matlab computations and to carry out the analytical calculations Matlab's Symbolic Math Toolbox is incapable of.

1.6 Key results

To summarize the result of the thesis, an analytical model of a flat two wheel vehicle was derived making it possible to obtain analytical expressions for the yaw velocity, lateral drift and lateral acceleration during high speed braking. This analytical model was verified by comparison with a more advanced, four wheel numerical vehicle model. Verification proved the analytical model to be slightly more oscillating but with the overall behaviour captured.

The impact of including different effects, such as combined slip and load transfer, in the vehicle and tyre model was also studied. Of all the effects studied, the lateral force steer and combined slip turned out to be the ones with the greatest influence on the outcome. To show the importance of the study the stability and controllability increase obtained by decreasing the vehicle velocity was analyzed.

1.7 Report outline

To help orient the reader in the structure of the thesis a brief description to indicate the progression of chapters and sections is presented below.

The thesis report lacks the classic report structure as the traditional method and result chapters are merged and then divided into three separate chapters. Therefore, the the report will start by presenting the governing theories upon which the work is based. This is followed by the merged method and result chapters leading to the final discussion and conclusion chapters. The reason for not using the report structure of separate method and result chapters is that all of the analytical derivations normally placed in the method chapter is to be seen as a significant part of the thesis result. This is why separating the analytical derivations and analyses into conventional method and result chapters becomes quite inept as a forced report structure.

2 Theory

This chapter contains information and descriptions of some basic theories needed for the study. Concepts and terminology of importance for understanding the progress of the thesis will be presented with a reader of a background of mechanical engineering in mind rather than a reader with a background focused on automotive studies. Hence the slight focus on presenting vehicle related terms and methods rather than mechanical and computational related ones.

2.1 Vehicle dynamics terminology

In this section terms and concepts used in the thesis will be introduced. The descriptions are kept brief as the reader is referred to the specified references for further descriptions.

2.1.1 Vehicle motion

The coordinate system used to determine the motion of the vehicle in this study is of Cartesian kind, oriented according to ISO8855 standard and shown in the figure below:

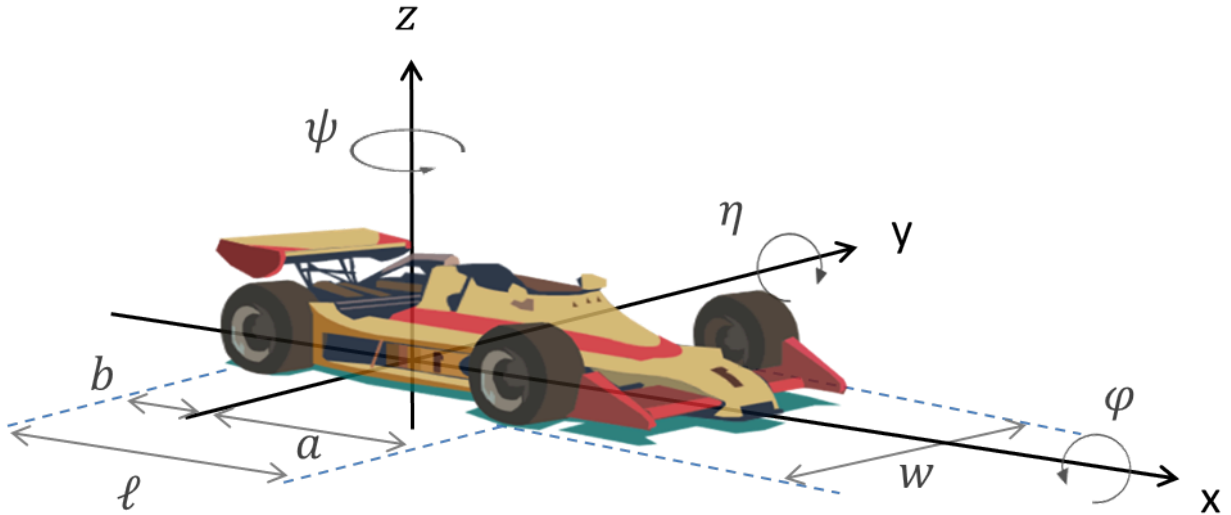


Figure 2.1: *Vehicle fixed Cartesian coordinate system*

Just as in aircraft and marine motion terminology, the rotational degrees of freedom of a vehicle are named yaw, pitch, and roll, shown as Ψ , η , and φ respectively in Figure 2.1. The longitudinal direction (along the x -axis) is defined as positive in the direction in which the front of the vehicle is pointing and the vertical direction (along the z -axis) in the direction normal to ground plane [8]. Figure 2.1 also illustrates the wheel base, ℓ , and distance to the front and rear axle, a and b , as well as the track width, w .

A term of great significance in vehicle terminology is the tyre *slip angle*, α . This is the angle between the longitudinal and actual direction of the velocity of the wheel hub, defined such that α is positive for positive lateral velocity. For one of the steering wheels, see Figure 2.2, the longitudinal velocity of the wheel hub is not necessarily in the same direction as the longitudinal velocity of the vehicle as the steer angle, δ , rotates the wheel around its own z -axis (assuming zero camber and caster angles in the steering geometry) [15].

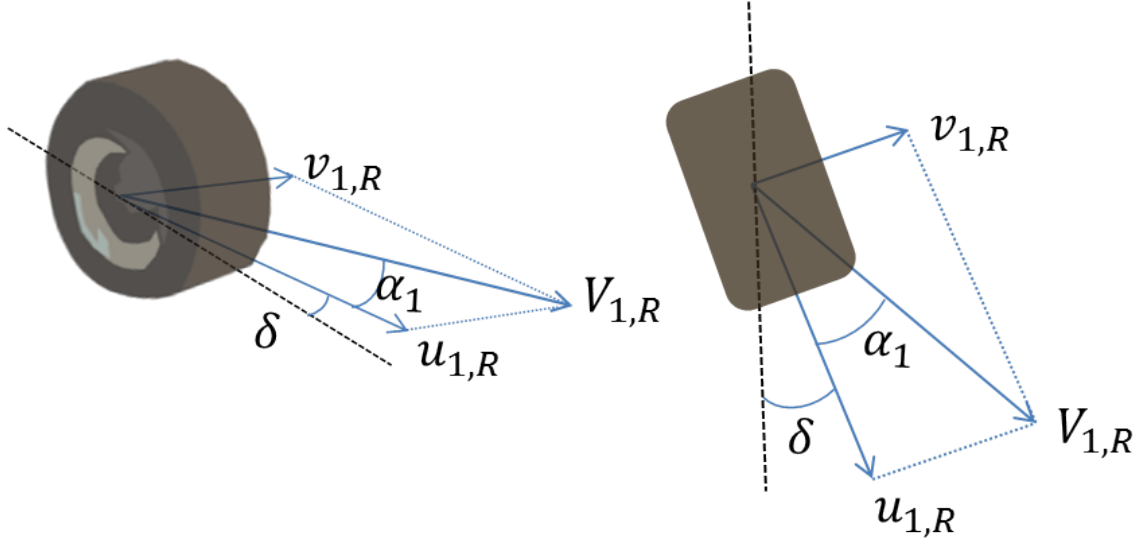


Figure 2.2: *Stere angle and slip angle illustration of right front wheel*

The figure shows the right front tyre of the vehicle shown in Figure 2.1, the dotted black line represents the x -axis of the vehicle. The camber and caster angle mentioned above determine the inclination of the wheel plane about the x -axis and the inclination of king-pin about the y -axis, i.e. the inclination of the axis around which the wheel is rotates when steered.

2.1.2 Tyre model

The handling and dynamical behaviour of a vehicle is greatly influenced by the vehicle's tyre properties since most, if not all, of the by driver controllable and desired environmental interactions are transferred through the tyres. The primary tasks of the tyres is to transfer forces in all three general coordinate directions (X - Y - Z) and to serve as a cushion of air isolating the vehicle from surface irregularities. This way the tyre carries vertical loads, transfers brake- and acceleration forces, generates lateral forces, and dampens vertical disturbances [15] [8].

As a tyre of a vehicle rolls along a flat, smooth surface several complex phenomenon occurs. Such as lateral and longitudinal wheel slip which gives rise to frictional forces trying to prevent the tyre from slipping, deformation of the tyre causing a non-constant tyre radius, and vibrations between the wheel rim and tyre. Several analytically and empirical mathematical models have been developed, each focusing on capturing and describing different phenomena, some of which mentioned previously [15].

One of the more well-known models is the often used semi-empirical model Magic Formula, see Equation 2.1. This is a function which describes the steady-state tyre side force as a function of the wheel slip angle, α_i , based on the vehicle specific parameters: Tyre stiffness factor B , curve shape factor C , peak value of the tyre force D , and the curve factor E [15].

$$F_{yi} = -D \sin \left(C \arctan \left\{ B\alpha_i - E(B\alpha_i - \arctan(B\alpha_i)) \right\} \right) \quad (2.1)$$

The minus sign in the expression for Magic Formula stated above is added due to the sign convention used in this thesis.

The typical appearance of the Magic formula plotted is shown in Figure 2.3.

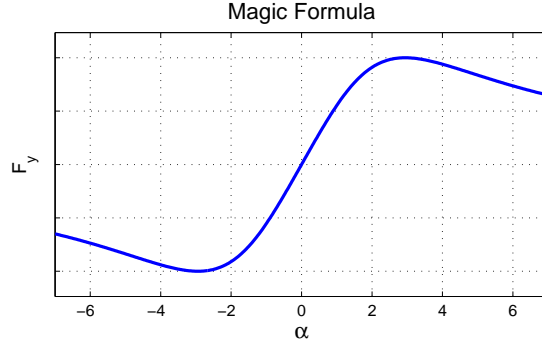


Figure 2.3: Typical shape the curve describing the lateral force for different slip angles using the Magic Formula

In the case of the vehicle travelling straight ahead or close to it, with only small slip angles present it can be argued that a linearised version of the Magic Formula can be used to simplify analytical computation significantly. Linearizing the Magic Formula the relation shown in Equation 2.2 is obtained.

$$F_{yi} = -C_{F\alpha i} \alpha_i \quad (2.2)$$

Here $C_{F\alpha i}$ is the effective cornering stiffness $C_{F\alpha i} = B \cdot C \cdot D$ obtained from linearising Magic Formula with respect to α . The lateral tyre force is linearly dependent in the slip angle, which as seen in Figure 2.3 is an appropriate approximation as the cornering stiffness $C_{F\alpha i}$ is the slope of the plotted curve for small slip angles.

To capture how the longitudinal tyre forces affect the tyre's ability to withstand lateral forces a method called *combined slip* is employed. Using this method the cornering stiffness is expressed as shown in the Equation below:

$$C_{F\alpha i}^* = C_{F\alpha i} \left(1 - \frac{1}{2} \left(\frac{F_{xi}}{\mu F_{zi}} \right)^2 \right) \quad (2.3)$$

This method of modelling the tyre properties takes in to account that the greater the longitudinal force which the tyre is subjected to the lesser lateral force it can absorb, which is the behaviour seen in tyre tests. $C_{F\alpha i}^*$ in Equation 2.3 is called the equivalent cornering stiffness and replaces $C_{F\alpha i}$ in the tyre model above to include the effect of combined slip [1].

As the combined slip tyre model shown in Equation 2.3 includes the normal force F_{zi} this model can take into account the effects of load transfer, i.e. that the normal force which the tyre experiences changes as the vehicle is cornering, braking, or accelerating. To further take this effect in to account the following formula for the cornering stiffness is used, derived from a simplified version of the Magic formula (Equation 2.1) [15].

$$C_{F\alpha i}^* = C_{F\alpha i} \sin \left(2 \arctan \left(\frac{F_{zi}}{F_{avr}} \right) \right) \quad (2.4)$$

where F_{avr} is the average static normal force acting on the tyres of the vehicle.

2.1.3 Steering effects

The handling characteristics of a vehicle is to a large extent determined by if the vehicle is understeered, neutrally steered, or oversteered, which is based on the relation between the vehicle's yaw angle and steer angle. For an understeered vehicle traveling with increasing velocity and with constant turning radius the steer angle must be increased as the velocity is increased for the turning radius to remain constant. For an oversteered vehicle the inverse of the relationship holds, the steer angle must be decreased as the velocity is increased for the turning radius to remain constant. If the vehicle would to be neutrally steered increased velocity does not

require any change in steer angle to keep the vehicle turning with constant turning radius. Whether or not a vehicle is understeered or oversteered is determined by its understeer gradient, ε , shown below [15].

$$\varepsilon = -\frac{mg(aC_{F\alpha 1} - bC_{F\alpha 2})}{\ell C_{F\alpha 1}C_{F\alpha 2}} \quad (2.5)$$

For an oversteered vehicle $\varepsilon < 0$, for an understeered $\varepsilon > 0$, and for an neutrally steered vehicle $\varepsilon = 0$. Which in other words gives that if the rear axle cornering stiffness is weaker than that of the front axle the vehicle will be oversteered and thus the vehicle will tend to turn more than what the driver implies by the steer angle input, and vice versa for an understeered vehicle.

One of the governing limitations of the project is that it is assumed that the driver of the vehicle does not steer the vehicle, i.e. there is no steer input via the steering wheel during the braking procedure. This however does not mean that the steer angle of vehicle's wheels are fixed. The lateral forces acting on the wheels and the pitching and rolling motion of the vehicle does in fact steer the wheels.

Due to the configuration of the vehicle's suspension and also due to the tyre dynamics, the equivalent point of attack for the force acting at the tyre surface contact is not located directly below the wheel hub. Therefore the lateral forces gives rise to a moment T_s , called self aligning moment or steering torque. The distance to the equivalent point of attack for the lateral forces, i.e. the lever for the lateral force, is called pneumatic trail, ξ_{Tr} , and is illustrated in Figure 2.4 [8].

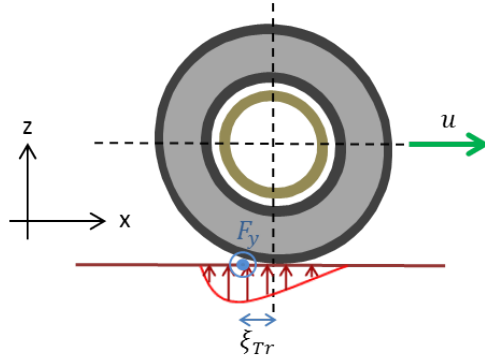


Figure 2.4: *Pneumatic trail, ξ_{Tr} , and contact patch force distribution for the tyre-surface interaction*

As mentioned, the pneumatic trail ξ_{Tr} together with the lateral forces acting on the wheels gives rise to a moment T_s which in turn yields the self aligning steer effect. This effect is amplified further as the vehicle experiences pitching and rolling motion due to the structure of the vehicle's suspension. For the case of small, constant lateral and longitudinal accelerations the combined outcome of these two effects can be expressed as the following steer angle change [1]:

$$\delta_{T_s} = (\kappa_1 + \kappa_2 a_x) a_y \quad (2.6)$$

The coefficients κ_1 and κ_2 are constants dependent on the configuration of the wheel suspension and steering system, see Equation 2.7.

$$\begin{aligned} \kappa_1 &= -\frac{\partial \delta}{\partial T_s} \xi_{Tr} \frac{bm}{\ell} \\ \kappa_2 &= -\frac{\partial \delta}{\partial T_s} \frac{\gamma_{bd} m}{2K_y} \frac{bm}{\ell} \end{aligned} \quad (2.7)$$

where ξ_{Tr} is the pneumatic trail illustrated in Figure 2.4, $\frac{\partial \delta}{\partial T_s}$ is the steer system compliance steer per unit steering torque, i.e. how easily the steering system is affected by the steering torque. γ_{bd} in the expression for κ_2 is the brake force distribution between the front and rear tyres and K_y the lateral stiffness of the tyre. Important to note is that the roll effects can be included in the expressions for κ_1 and κ_2 , these effects are

however excluded in the expressions stated in the equations above.

It must be noted that this model for steer angle change is only valid for the case of small, stationary lateral and longitudinal accelerations. Therefore, this model cannot cope with large or vigorously fluctuating accelerations. For small and slow oscillations around the stationary values the model can be assumed to capture the dynamic behaviour of the vehicle [1].

2.1.4 Aerodynamic lift effects

As a vehicle travels at high speed the aerodynamic effects caused by the interaction between the vehicle body and the air it passes through cannot be neglected. The most obvious effect is the lateral drag force that the vehicle must overcome to maintain its velocity. However, this effect is of little importance in this study as the lateral forces acting on the vehicle, i.e. the braking forces, are assumed to be known and the drag force will only contribute to the longitudinal forces. An aerodynamic effect of significance for the study which beforehand cannot be neglected is the aerodynamic lift force.

The aerodynamic lift force is generated by the pressure gradient from the top to the bottom of the vehicle. As this force effects the normal forces between the vehicle's tyres and the road surface it strongly effects stability of the vehicle, hence it is importance for this thesis. The effect can have positive or negative effects on the stability as the generated lift force can be either positive or negative depending on the shape of the vehicle's body. For example, spoilers, underbody pans, and aerofoils can be mounted on a vehicle to decrease the lift force or even cause a negative lift force, i.e. a down force. The generated lift force is governed by the following equation [10]:

$$\Delta F_{z,i,lift} = \frac{1}{2} \rho u^2 C_{L,i} A \quad (2.8)$$

where ρ is the air density, $C_{L,i}$ the lift force coefficient for the i :th, and A the frontal area of the vehicle. The lift force coefficient is dependent on the shape of the vehicle's body, 0.3 to 0.5 is a normal span for the lift force coefficient of modern cars [10].

2.1.5 Quasi steady state vehicle motion

Performing an analytical study of the fundamental characteristics of vehicle motion based on the equations of motion is tedious if the full dynamic behavior is to be considered. Therefore, some modifications are needed for analytical solvability. When a vehicle undergoes a severe braking procedure with constant braking forces, the vehicle speed will change and a steady-state condition will not be fulfilled. A remedy to this is to only consider short periods of time where the velocity change due to braking may be neglected, e.g. when the vehicle is travelling at high speed, and a assumption of a steady-state with constant longitudinal and lateral acceleration is possible. This is called a Quasi-steady-state motion, or a *Quasi-static motion* [1].

2.2 Lagrange equation for quasi-coordinates

Determining the motion of a vehicle using a global reference frame is often disadvantageous when it comes to specifying the vehicle's velocity and acceleration. As an example, the speed, i.e. the norm of the global velocity vector, experienced by the driver of the vehicle may be constant but the components of the global velocity vector may vary (assuming planar motion). Therefore using the global velocity vector components for specifying the vehicle's motion is not optimal from the driver's point of view. The driver operates the vehicle by continuous inputs based on the response experienced from within the vehicle therefore it is beneficial to use a dynamic, vehicle fixed reference frame to determine the velocity and acceleration of the vehicle, i.e. a *quasi-coordinate system*. For this reason the governing equations of motion, Lagrange's equations, for a vehicle must be expressed in this system, a Cartesian coordinate system attached to the vehicle. This can be seen as a more "natural" way of expressing the motion of a moving body [13].

Lagrange's equations of motion for a set of generalized coordinates q_k ($k = 1, 2, \dots, n$), which can be regarded as *true coordinates*, are written as:

$$\frac{d}{dt} \left(\frac{\partial \mathcal{L}}{\partial \dot{q}_i} \right) - \frac{\partial \mathcal{L}}{\partial q_i} = Q_i \quad (2.9)$$

with \mathcal{L} , the Lagrangian, given as:

$$\mathcal{L} = T - V \quad (2.10)$$

where T is the kinetic energy and V the potential energy. It is in some special occasions useful to derive equations of motion which are not restricted to the true coordinates q_k , but to a set of variables ω_s ($s = 1, 2, \dots, n$), see Equation 2.11, that consists of linear independent combinations of the generalized velocities \dot{q}_k . This set of variables are called *quasi-coordinates*. These coordinates cannot be integrated to obtain the true coordinates of the body.

$$\omega_s = \alpha_{1s}\dot{q}_1 + \alpha_{2s}\dot{q}_2 + \dots + \alpha_{ns}\dot{q}_n \quad (2.11)$$

where α_{ns} are known functions of the generalized coordinates q_k .

Equation 2.11 is written using Einstein's index notation which gives the expression shown below:

$$\omega_s = \alpha_{ks}\dot{q}_k \quad (2.12)$$

Now, introducing β_{kp} such that the time derivatives of the generalized coordinates can be written as:

$$\dot{q}_k = \beta_{kp}\omega_p \quad (2.13)$$

For Equation 2.13 to be valid, following must hold:

$$\omega_s = \alpha_{ks}\dot{q}_k = \alpha_{ks}\beta_{kp}\omega_p = \delta_{sp}\omega_p = \omega_s \quad (2.14)$$

i.e. $\alpha_{ks}\beta_{kp} = \delta_{sp}$, which is the Kronecker's delta.

This enables the Lagrangian, $\mathcal{L}(q_k, \dot{q}_k)$, to be written as a function of the generalized coordinates, q_k , and the quasi-coordinates, ω_s , i.e.

$$\bar{\mathcal{L}}(q_k, \omega_s) = \bar{T} - V \quad (2.15)$$

compared to $\mathcal{L}(q_k, \dot{q}_k) = T - V$. With the Lagrangian expressed as $\bar{\mathcal{L}}(q_k, \omega_s)$, Equation 2.9 is rewritten for quasi-coordinates using the chain-rule for the first term of the left hand side (LHS):

$$\frac{\partial \mathcal{L}}{\partial \dot{q}_i} = \frac{\partial \bar{\mathcal{L}}}{\partial \omega_s} \frac{\partial \omega_s}{\partial \dot{q}_i} = \left\{ \text{eq. 2.12} \right\} = \alpha_{is} \frac{\partial \bar{\mathcal{L}}}{\partial \omega_s} \quad (2.16)$$

The time derivative then becomes:

$$\frac{d}{dt} \left(\frac{\partial \mathcal{L}}{\partial \dot{q}_i} \right) = \alpha_{is} \frac{d}{dt} \left(\frac{\partial \bar{\mathcal{L}}}{\partial \omega_s} \right) + \dot{\alpha}_{is} \frac{\partial \bar{\mathcal{L}}}{\partial \omega_s} \quad (2.17)$$

Since α_{is} only consists of known functions of the generalized coordinates, the time-derivative of this term can be written as:

$$\dot{\alpha}_{is} = \frac{\partial \alpha_{is}}{\partial q_k} \dot{q}_k \quad (2.18)$$

This together with Equation 2.13 becomes:

$$\dot{\alpha}_{is} = \beta_{kj}\omega_j \frac{\partial \alpha_{is}}{\partial q_k} \quad (2.19)$$

Rewriting the second term of the left hand side of Equation 2.9 using the Lagrangian expressed as $\bar{\mathcal{L}}(q_k, \omega_s)$ gives the following expression:

$$\begin{aligned}\frac{\partial \mathcal{L}}{\partial q_i} &= \frac{\partial \bar{\mathcal{L}}}{\partial q_i} + \frac{\partial \bar{\mathcal{L}}}{\partial \omega_s} \frac{\partial \omega_s}{\partial q_i} = \left\{ \text{eq. 2.12, Note: } \alpha_{is} = \alpha_{is}(q_k) \right\} \\ &= \frac{\partial \bar{\mathcal{L}}}{\partial q_i} + \frac{\partial \bar{\mathcal{L}}}{\partial \omega_s} \frac{\partial \alpha_{ks}}{\partial q_i} \dot{q}_k = \left\{ \text{eq. 2.13} \right\} = \frac{\partial \bar{\mathcal{L}}}{\partial q_i} + \frac{\partial \bar{\mathcal{L}}}{\partial \omega_s} \frac{\partial \alpha_{ks}}{\partial q_i} \beta_{kl} \omega_l\end{aligned}\quad (2.20)$$

Inserting Equations 2.17, 2.18 and 2.20 into Equation 2.9 the following is obtained:

$$\begin{aligned}\alpha_{is} \frac{d}{dt} \left(\frac{\partial \bar{\mathcal{L}}}{\partial \omega_s} \right) + \beta_{kj} \omega_j \frac{\partial \alpha_{is}}{\partial q_k} \frac{\partial \bar{\mathcal{L}}}{\partial \omega_s} - \frac{\partial \bar{\mathcal{L}}}{\partial q_i} - \beta_{kl} \omega_l \frac{\partial \bar{\mathcal{L}}}{\partial \omega_s} \frac{\partial \alpha_{ks}}{\partial q_i} &= Q_i \Rightarrow \\ \Rightarrow \alpha_{is} \frac{d}{dt} \left(\frac{\partial \bar{\mathcal{L}}}{\partial \omega_s} \right) + \beta_{kj} \omega_j \left(\frac{\partial \alpha_{is}}{\partial q_k} - \frac{\partial \alpha_{ks}}{\partial q_i} \right) \frac{\partial \bar{\mathcal{L}}}{\partial \omega_s} - \frac{\partial \bar{\mathcal{L}}}{\partial q_i} &= Q_i\end{aligned}\quad (2.21)$$

To simplify Equation 2.21 the expression is multiplied by β_{im} :

$$\beta_{im} \alpha_{is} \frac{d}{dt} \left(\frac{\partial \bar{\mathcal{L}}}{\partial \omega_s} \right) + \beta_{im} \beta_{kj} \omega_j \left(\frac{\partial \alpha_{is}}{\partial q_k} - \frac{\partial \alpha_{ks}}{\partial q_i} \right) \frac{\partial \bar{\mathcal{L}}}{\partial \omega_s} - \beta_{im} \frac{\partial \bar{\mathcal{L}}}{\partial q_i} = \beta_{im} Q_i = N_m \quad (2.22)$$

This equation can be reduced further by use of Equation 2.14:

$$\frac{d}{dt} \left(\frac{\partial \bar{\mathcal{L}}}{\partial \omega_m} \right) + \beta_{im} \beta_{kj} \omega_j \left(\frac{\partial \alpha_{is}}{\partial q_k} - \frac{\partial \alpha_{ks}}{\partial q_i} \right) \frac{\partial \bar{\mathcal{L}}}{\partial \omega_s} - \beta_{im} \frac{\partial \bar{\mathcal{L}}}{\partial q_i} = N_m \quad (2.23)$$

It is here useful to introduce γ_{is}

$$\gamma_{is} = \beta_{kj} \omega_j \left(\frac{\partial \alpha_{is}}{\partial q_k} - \frac{\partial \alpha_{ks}}{\partial q_i} \right) \quad (2.24)$$

The final expression for Lagrange's equations with quasi-coordinates then becomes

$$\begin{cases} \frac{d}{dt} \left(\frac{\partial \bar{\mathcal{L}}}{\partial \omega_m} \right) + \beta_{im} \gamma_{is} \frac{\partial \bar{\mathcal{L}}}{\partial \omega_s} - \beta_{im} \frac{\partial \bar{\mathcal{L}}}{\partial q_i} = N_m \\ N_m = \beta_{im} Q_i \end{cases} \quad (2.25)$$

with β_{im} obtained from Equation 2.13 and γ_{is} from Equation 2.24.

2.3 Differential equations

For the general case Lagrange's equations for quasi-coordinates (Equation 2.25) generates a system of differential equations, i.e. a system of equations containing variables, functions, and different order derivatives of these functions. This section presents the general methodology for how differential equations are classified and solved using different techniques.

2.3.1 Differential equation classification

Differential equations are equations which describe systems governed by their current state and rate change of that state. Past states can also be connected and influence the current state of the system. Thereby many phenomena, both physical and abstract, can be modelled using differential equations [12]. To enable a concentrated study of the subject matter where the system is governed by differential equations classifying the equations is often beneficial. The main classifications of differential are listed below [17]:

- ordinary or partial
- linear or nonlinear
- homogenous or nonhomogeneous
- autonomous or nonautonomous
- first order, second order, ... , n:th order

A differential equation is said to be ordinary if the derivatives of the unknown function are ordinary derivatives, $\frac{d}{dx}$, partial if the unknown function derivatives are partial, $\frac{\partial}{\partial x}$. Linear or nonlinear meaning if solutions to the differential equation can be added together to obtain another valid solution to the equation, the differential equation can still be ordinary or partial. Whether or not a differential equation is homogeneous or nonhomogeneous simply means if the equation has a zero or nonzero right hand side, with the right hand side equalling zero making the differential equation homogeneous. If the right hand side does not explicitly depend on the independent variable of the differential equation the equation is said to be autonomous. The order of the differential equation is the order of the highest appearing derivative of the unknown function [17].

Closer analysis of nonelementary differential equations requires more precise and detailed classification of the equation to determine how and if it can be solved. If the coefficients of the differential equation are constant or not is a key factor in determining how the differential equation should be treated. If the coefficients are varying then their composition and complexity is of great importance for the analytical solvability of the differential equation. Depending on the appearance of the coefficients and the order of the differential equation, the solution may consist of different mathematical functions. Of special interest for this study is the case for which the differential equation is solved using Bessel functions.

2.3.2 Linearization of differential equation

When analysing a dynamic non-linear system the easiest way of simplifying the system to enable and facilitate analytical computations is to approximate the non-linear system as a linear one, i.e. linearizing it. One method of linearization is to assume that the system of equations $\mathbf{y} = \mathbf{f}(\mathbf{x})$, or single equation $y = f(x)$, varies with small fluctuations around an operating point, or reference state, \mathbf{x}_0 . This is done by assuming, or knowing, the value of the parameters in \mathbf{x}_0 to be *approximately* constant, i.e. fluctuating around a fix value with a small amplitude as shown in Equation 2.26 [6].

$$(x_0)_i = x_i^* + \tilde{x}_i \quad (2.26)$$

$(x_0)_i$ is an arbitrary variable in \mathbf{x}_0 , x_i^* its stationary value and \tilde{x}_i a small fluctuation around this stationary value. The key in the simplifications is knowing that the fluctuations are small since the product of two small terms is said to be approximately zero. Cosine and sine are linearised to the first order, hence cosine of a small angle approximately unity, $\cos(\tilde{x}_i) \approx 1$, and sine of a small angle approximately the angle itself, $\sin(\tilde{x}_i) \approx \tilde{x}_i$. Important to notice is that when using Lagrange's Equations to establish the motion equations the terms must be expanded such that quadratic terms are included in the simplified expressions, for example $\cos(\tilde{x}_i) \approx 1 - \frac{1}{2}\tilde{x}_i^2$.

When applied to a differential equation this linearization scheme often enables the equation to be solved analytically by simple means as the time derivative of a small fluctuation also is assumed to be small. This elimination of products of small terms often simplifies the expression significantly. All components of the operating point \mathbf{x}_0 does not necessarily have to be able to be rewritten as a constant and a fluctuating part, as in Equation 2.26, for the linearization to be possible. This approximation may only be valid for some \mathbf{x}_0 components, the system is then said to be linear with respect to those components.

2.3.3 State space representation

Rewriting a differential equation of higher order to a system of first order differential equations, possibly by linearization (see Equation 2.26), provides a compact and simple representation of an otherwise complicated equation. This is especially useful when analysing controllability and stability of a system and also when using numerical solvers to solve the differential equations [6].

A mechanical system with damped oscillations is represented by the following mathematical model where ω and ξ are the eigenfrequency and damping of the system.

$$\ddot{x}(t) + 2\xi\omega\dot{x}(t) + \omega^2x(t) = F(t) \quad (2.27)$$

To be able to rewrite the second order differential equation as a system of first order differential equations the following parameters are introduced:

$$\mathbf{z} = \begin{bmatrix} z_1(t) \\ z_2(t) \end{bmatrix} = \begin{bmatrix} x(t) \\ \dot{x}(t) \end{bmatrix} \quad (2.28)$$

This enables Equation 2.27 to be written as state space representation:

$$\begin{bmatrix} \dot{z}_1(t) \\ \dot{z}_2(t) \end{bmatrix} = \underbrace{\begin{bmatrix} 0 & 1 \\ -\omega^2 & -2\xi\omega \end{bmatrix}}_{\mathbf{A}} \begin{bmatrix} z_1(t) \\ z_2(t) \end{bmatrix} + \underbrace{\begin{bmatrix} 0 & 0 \\ 0 & 1 \end{bmatrix}}_{\mathbf{B}} \begin{bmatrix} 0 \\ F(t) \end{bmatrix} \quad (2.29)$$

The equation can now be written in matrix form as shown in Equation 2.30.

$$\dot{\mathbf{z}} = \mathbf{A} \cdot \mathbf{z} + \mathbf{B} \cdot \mathbf{u} \quad (2.30)$$

In the general case both the system matrix, \mathbf{A} , and the input matrix, \mathbf{B} , can be time varying as well.

2.3.4 Ordinary differential equation

If the system of interest is described by a single differential equation, or a system of differential equations, and this equation is an ordinary differential equation then the equation can be generally formulated as follows:

$$F\left(x, y, \frac{dy}{dx}, \dots, \frac{d^n y}{dx^n}\right) = R(x) \quad (2.31)$$

where $y = y(x)$ is the unknown function and x is the free variable. The solution, if the differential equation is linear, is found by solving both the nonhomogeneous equation, see Equation 2.31, and its corresponding homogeneous equation, i.e. $R(x) = 0$, see Equation 2.32.

$$F\left(x, y, \frac{dy}{dx}, \dots, \frac{d^n y}{dx^n}\right) = 0 \quad (2.32)$$

These two solutions, the particular and homogeneous solution, are now added together to obtain the total solution of the linear differential equation.

2.3.4.1 Homogeneous solution, constant coefficients

As mentioned previously, the general form of a homogeneous differential equation is obtained by putting its right hand side, $R(x)$, to zero. For illustrative purposes it is now assumed that the left hand side is a linear differential equation of second order with constant coefficients as shown below:

$$\ddot{y}(t) + C_1\dot{y}(t) + C_2y(t) = 0 \quad (2.33)$$

This equation is solved by first writing the characteristic form of the equation and solving roots of the equation. For this type of differential equation, the characteristic equation will have the following form:

$$\lambda^2 + C_1\lambda + C_2 = 0 \quad (2.34)$$

The resulting roots of Equation 2.34, λ_1 and λ_2 , are then used to describe the solution of Equation 2.33 as:

$$y(t) = D_1 e^{\lambda_1 t} + D_2 e^{\lambda_2 t} \quad (2.35)$$

where D_1 and D_2 are constants which are determined using initial conditions.

2.3.4.2 Homogeneous solution, variable coefficients

For the case of the left hand side of Equation 2.32 having nonconstant coefficients its solution is strongly dependent of the complexity of these coefficients. Given that the unknown function, $y(x)$, the free variable, x , and the coefficients can be rewritten to the form shown in Equation 2.36 the solution of the equation can be formulated using Bessel functions.

$$x^2 \frac{d^2 y}{dx^2} + (2\tilde{p} + 1)x \frac{dy}{dx} + (\tilde{\alpha}^2 x^{2\tilde{r}} + \tilde{\beta}^2)y = 0 \quad (2.36)$$

This equation is a version of the so called Bessel differential equation. The reason for rewriting a differential equation on this form is that the solution for this is known to be as follows [7]:

$$y = x^{-\tilde{p}} \left[C_1 \mathbf{J}_{\tilde{q}/\tilde{r}} \left(\frac{\tilde{\alpha}}{\tilde{r}} x^{\tilde{r}} \right) + C_2 \mathbf{Y}_{\tilde{q}/\tilde{r}} \left(\frac{\tilde{\alpha}}{\tilde{r}} x^{\tilde{r}} \right) \right] \quad (2.37)$$

where C_1 and C_2 are constants from the integration determined by initial conditions on y . $\mathbf{J}_{\tilde{q}/\tilde{r}}$ and $\mathbf{Y}_{\tilde{q}/\tilde{r}}$ are the Bessel functions of first and second order respectively with $\tilde{q} = \sqrt{\tilde{p}^2 - \tilde{\beta}^2}$.

2.3.4.3 Particular differential equation solution

The particular solution is any solution satisfying the nonhomogeneous differential equation, i.e. Equation 2.31, and is usually obtained from a qualified guess. For a damped system the behaviour of the solution to a dynamical system is after some time completely governed by the particular solution, i.e. the homogeneous solution will have died out. When this time occurs depends on the systems characteristics [5]. Since completely undamped system only exists theoretically, all real life dynamic systems behave as aforesaid.

2.4 Stability definition

Before an analysis of a specific vehicle model's stability can be carried out a clear definition for the concept of stability must be determined. The definition of vehicle stability is not easily determined and it is not necessarily clear what is meant by stability in the vehicle terminology. Whereas the definition of stability in strict mathematical terms is clearly defined, it is not always usable in vehicle dynamics.

In a purely mathematical definition a system is asymptotically stable if all solutions approaches zero as the independent variable approaches infinity and unstable if the solutions grows towards infinity. There are several methods and mathematical theories to determine the stability of a function or system of coupled functions, for example Lyapanov stability theory and Routh-Hurwitz stability theory [5]. The mathematical definitions of stability applied to vehicle dynamics in terms of how the vehicle behaves when the independent variable, usually time, approaches infinity is of little use in vehicle stability analysis, as the time spans analysed rarely approaches infinity.

As mentioned, in vehicle dynamics the stability term has a broad meaning. It can be defined as whether or not large lateral slip is present at any axle [8], or defined by measuring the controllable region in which the driver can operate the vehicle safely [14]. Since this study considers high speed straight line braking the stability is determined by measuring the lateral drift (Y-direction movement) during the braking procedure and by analysing the operating conditions of the vehicle. During the brake procedure the system is excited by an initial disturbance or an continuous disturbance during the entire braking procedure.

In the global coordinate system (X - Y - Z system) the lateral drift is represented by the Y -position of the vehicle, i.e. the vehicle's lateral position on the road. The reason that this stability condition alone is insufficient for this study is that the vehicle's operating conditions at the end of, and also during, the deceleration is of

great importance for the controllability of the vehicle after the braking procedure and also for how the driver experiences the situation. For example, while the vehicle may be kept within its lane during the deceleration it might have spun around and therefore the deceleration cannot be seen as stable. When it comes to the driver's experience during the deceleration it is difficult to quantify conditions to be fulfilled since this is entirely subjective. But these conditions are not to be overlooked as the driver's reactions and reflexes during the deceleration might add to the severeness of the situation and cause more harm than good to the vehicle's ability to maintain within its lane. Therefore experiences from test drivers is used to determine limits on the yaw rate and lateral acceleration to avoid negative effects of driver vehicle interaction.

3 General equations of motion for a vehicle

In the following chapter the governing motion equations for a vehicle will be derived using a simplified four wheel model of a vehicle. This model is then simplified to obtain the required analytical solvability.

3.1 Derivation of motion equations for a basic four wheel model

Following the methodology of quasi-coordinate Lagrange equations, derived in Section 2.2, the equations of motion is in this chapter derived for the simple four wheel model of a vehicle shown in Figure 3.1.

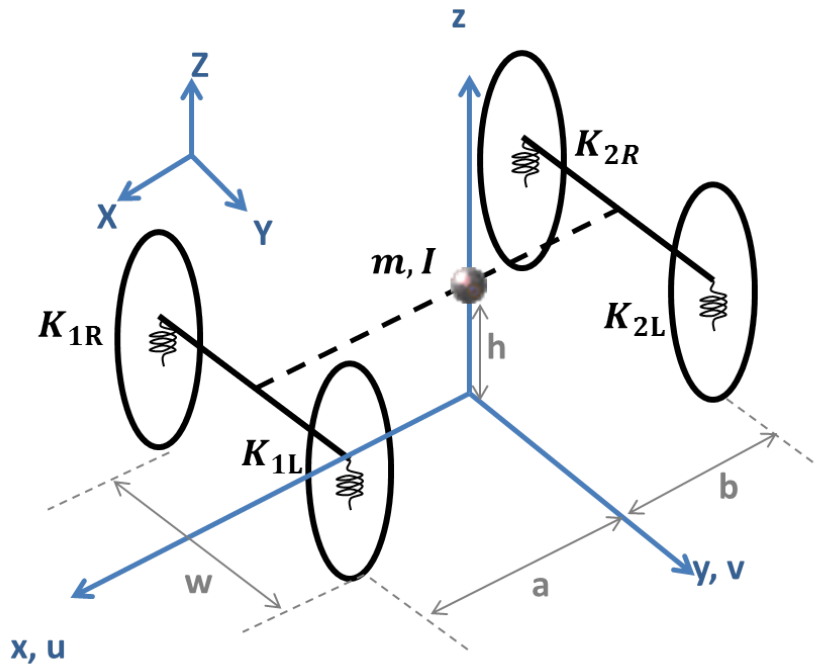


Figure 3.1: Schematic figure of a simple four wheeled vehicle model

The vehicle is assumed to be a rigid body with its center of mass located at the height h above the ground plane, a distance a from the front axle and b from the rear axle, and at the center of the vehicle laterally. The vehicle body is attached to the wheel hubs via springs and dampers, the dampers are not illustrated in the figure above. The rotational effects of the wheels are omitted from the analysis.

The motion of the vehicle model is governed by five equations of motion, two governing the planar motion and three governing the rotational degrees of freedom. The sixth degree of freedom in the general case, translational motion along the z -axis, is of no use in the analysis since the vehicle is assumed to travel on a flat, smooth road surface. Therefore, the vertical degree of freedom is only considered to obtain the change in potential energy, i.e. how the height of the center of mass changes as the vehicle experiences pitching and rolling motion. The planar motion and yaw-rotational velocity are expressed using quasi-coordinate Lagrange equations and the roll and pitch motion are expressed using classical Lagrangian mechanics.

From Figure 3.1 the quasi-coordinates, as given by Equation 2.11, can be expressed in time derivatives of the general coordinates as stated in the following expression:

$$\begin{cases} u(t) = \dot{X}(t) \cos(\Psi(t)) - \dot{Y}(t) \sin(\Psi(t)) \\ v(t) = \dot{X}(t) \sin(\Psi(t)) + \dot{Y}(t) \cos(\Psi(t)) \\ r(t) = \dot{\Psi}(t) \end{cases} \quad (3.1)$$

where XYZ are the global coordinates illustrated in Figure 3.1. Equation 3.1 is now rewritten on matrix form:

$$\underbrace{\begin{bmatrix} u \\ v \\ r \end{bmatrix}}_{\omega} = \underbrace{\begin{bmatrix} \cos(\Psi) & -\sin(\Psi) & 0 \\ \sin(\Psi) & \cos(\Psi) & 0 \\ 0 & 0 & 1 \end{bmatrix}}_{\alpha^T} \underbrace{\begin{bmatrix} \dot{X} \\ \dot{Y} \\ \dot{\Psi} \end{bmatrix}}_q \quad (3.2)$$

To determine the equations of motion using Equation 2.25 the quasi coordinate variables β and γ needs to be computed from Equation 2.13 and Equation 2.24 respectively:

$$\beta = (\alpha^T)^{-1} = \begin{bmatrix} \cos(\Psi) & -\sin(\Psi) & 0 \\ \sin(\Psi) & \cos(\Psi) & 0 \\ 0 & 0 & 1 \end{bmatrix} \quad (3.3)$$

$$\gamma = \begin{bmatrix} -r \sin(\Psi) & -r \cos(\Psi) & 0 \\ r \cos(\Psi) & -r \sin(\Psi) & 0 \\ -v & u & 0 \end{bmatrix} \quad (3.4)$$

Now, using Equation 2.25 the equations of motion are expressed in quasi-coordinates:

$$\frac{d}{dt}(\tilde{\nabla}\bar{\mathcal{L}}) + \beta^T \gamma \tilde{\nabla}\bar{\mathcal{L}} - \beta^T \nabla\bar{\mathcal{L}} = N \quad (3.5)$$

with

$$\tilde{\nabla} = \begin{bmatrix} \frac{\partial}{\partial u} \\ \frac{\partial}{\partial v} \\ \frac{\partial}{\partial r} \end{bmatrix} \quad \nabla = \begin{bmatrix} \frac{\partial}{\partial X} \\ \frac{\partial}{\partial Y} \\ \frac{\partial}{\partial Z} \end{bmatrix} \quad N = \begin{bmatrix} N_x \\ N_y \\ N_r \end{bmatrix} \quad (3.6)$$

For the remaining two motion equations, the equations governing the roll and pitch angles, classical Lagrangian mechanics is used as shown in the equation below:

$$\frac{d}{dt}\left(\frac{\partial\bar{\mathcal{L}}}{\partial\dot{q}}\right) - \frac{\partial\bar{\mathcal{L}}}{\partial q} = Q \quad (3.7)$$

The five equations of motion for the four wheel vehicle model shown in Figure 3.1 are now obtained from Equations 3.5 and 3.7:

$$\frac{d}{dt}\left(\frac{\partial\bar{\mathcal{L}}}{\partial\dot{u}}\right) - r\frac{\partial\bar{\mathcal{L}}}{\partial v} = Q_u \quad (3.8a)$$

$$\frac{d}{dt}\left(\frac{\partial\bar{\mathcal{L}}}{\partial\dot{v}}\right) + r\frac{\partial\bar{\mathcal{L}}}{\partial u} = Q_v \quad (3.8b)$$

$$\frac{d}{dt}\left(\frac{\partial\bar{\mathcal{L}}}{\partial\dot{r}}\right) - v\frac{\partial\bar{\mathcal{L}}}{\partial u} + u\frac{\partial\bar{\mathcal{L}}}{\partial v} = Q_r \quad (3.8c)$$

$$\frac{d}{dt}\left(\frac{\partial\bar{\mathcal{L}}}{\partial\dot{\varphi}}\right) - \frac{\partial\bar{\mathcal{L}}}{\partial\varphi} = Q_\phi \quad (3.8d)$$

$$\frac{d}{dt}\left(\frac{\partial\bar{\mathcal{L}}}{\partial\dot{\eta}}\right) - \frac{\partial\bar{\mathcal{L}}}{\partial\eta} = Q_\eta \quad (3.8e)$$

The Lagrangian is obtained from Equations 2.15 and 2.10 with the kinetic energy, T , is computed as shown in Equation 3.9.

$$\bar{T} = \frac{1}{2}v_{CoM}^T m v_{CoM} + \frac{1}{2}\Omega_R^T I \Omega_R \quad (3.9)$$

The velocity for the vehicle's center of mass, \mathbf{v}_{CoM} , and its rotational velocity, $\mathbf{\Omega}$, are shown in the following expressions:

$$\begin{aligned}\mathbf{v}_{CoM} &= \mathbf{v}_{xyz} + \mathbf{\Omega} \times \mathbf{r}_{pos} \\ \mathbf{\Omega} &= [\dot{\varphi} \quad \dot{\eta} \quad r]^T \\ \mathbf{\Omega}_R &= \begin{bmatrix} 1 & 0 & 0 \\ 0 & \cos(\varphi) & -\sin(\varphi) \\ 0 & \sin(\varphi) & \cos(\varphi) \end{bmatrix} \begin{bmatrix} \cos(\eta) & 0 & \sin(\eta) \\ 0 & 1 & 0 \\ -\sin(\eta) & 0 & \cos(\eta) \end{bmatrix} \mathbf{\Omega}\end{aligned}\quad (3.10)$$

The reason for transforming the rotational velocity vector, $\mathbf{\Omega}$, to $\mathbf{\Omega}_R$ is that the inertia matrix \mathbf{I} is expressed for the vehicle's body and therefore the rotational velocity vector must be expressed in the vehicle body's local coordinate system, i.e. rotated an angle φ around the x -axis and an angle η around the y -axis. The velocity of the origin of the xyz coordinate system, \mathbf{v}_{xyz} , and the position vector, \mathbf{r}_{pos} , are computed according to Equation 3.11.

$$\begin{aligned}\mathbf{v}_{xyz} &= [u \quad v \quad 0]^T \\ \mathbf{r}_{pos} &= h \cdot [\sin(\varphi) \quad \sin(\eta) \quad \cos(\eta) \cos(\varphi)]^T\end{aligned}\quad (3.11)$$

The potential energy of the system, V , is determined by the height of the vehicles center of mass and by the compression of the springs in the vehicles suspensions system. The expression for this becomes as follows:

$$V = mgh \cos(\eta) \cos(\varphi) + \frac{1}{2}K_{1R}(\Delta_{K_{1R}})^2 + \frac{1}{2}K_{1L}(\Delta_{K_{1L}})^2 + \frac{1}{2}K_{2R}(\Delta_{K_{2R}})^2 + \frac{1}{2}K_{2L}(\Delta_{K_{2L}})^2 \quad (3.12)$$

Here K_{1R} is the spring coefficient of the right spring of the front axel and $\Delta_{K_{1R}}$ the compression of the same spring, and vice versa for the remaining springs. The spring compression is illustrated in Figure 3.2.

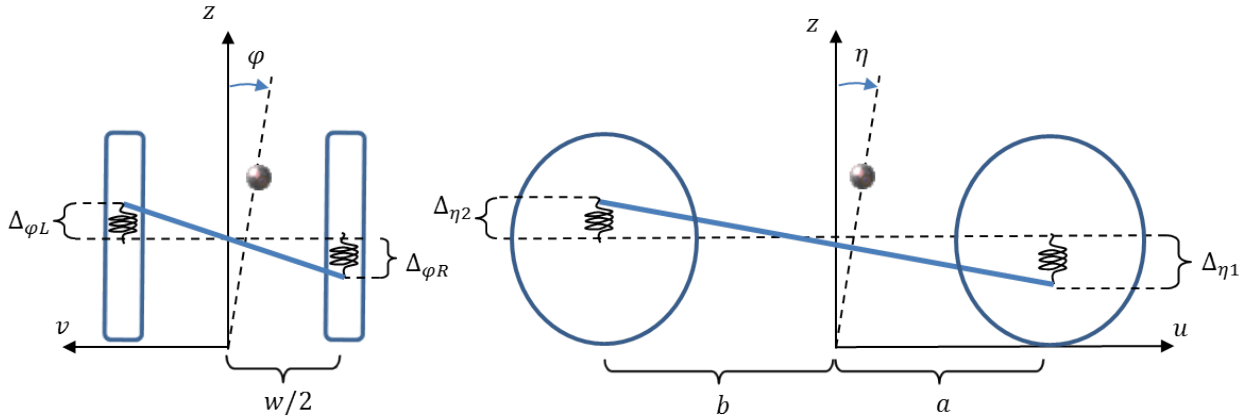


Figure 3.2: Compression of front and rear, left and right springs

From the geometric relations shown in the figure the spring compressions can be determined. As an example, the front right tyre will experience the following compression due to the roll- and pitch motions:

$$\Delta_{K_{2R}} = R(1 - \cos(\eta)) + a \sin(\eta) + R(1 - \cos(\varphi)) + \frac{w}{2} \sin(\varphi) = \left\{ \eta, \varphi \ll 1 \right\} \approx a\eta + \frac{w}{2}\varphi \quad (3.13)$$

Where R is the wheel radius. Using the same principle for the remaining springs the potential energy becomes as follows:

$$\begin{aligned}V &= \frac{1}{8} \left(8mgh \cos(\eta(t)) \cos(\varphi(t)) + 4\eta(t)^2 \left(a^2(K_{1L} + K_{1R}) + b^2(K_{2L} + K_{2R}) \right) + \right. \\ &\quad \left. 4w\eta(t)\varphi(t) \left(a(K_{1R} - K_{1L}) + b(K_{2L} - K_{2R}) \right) + w^2\varphi(t)^2 \left(K_{1L} + K_{1R} + K_{2L} + K_{2R} \right) \right)\end{aligned}\quad (3.14)$$

Knowing both the kinetic energy, \bar{T} , and the potential energy, V , the left hand side of the Lagrange's equations can be computed by inserting the Lagrangian ($\bar{\mathcal{L}} = \bar{T} - V$) into Equation 3.8. Which leaves the right hand side of Lagrange's equations, the generalized forces Q_i , to be determined for the motion equations to be fully known. These generalised forces are derived from the free body diagram of the model shown in Figure 3.3.

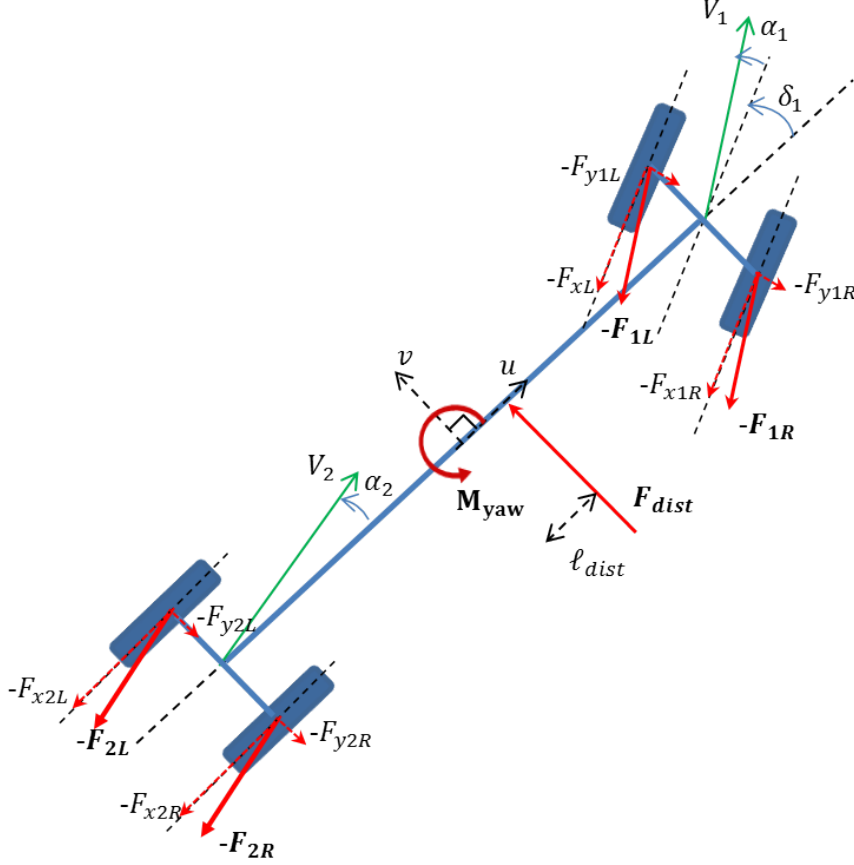


Figure 3.3: Free body diagram of the four wheel model seen from above

Using the principle of virtual work which yields the following results:

$$Q_u = F_{x2L} + F_{x2R} + (F_{x1L} + F_{x1R}) \cos(\delta) - (F_{y1L} + F_{y1R}) \sin(\delta) \quad (3.15a)$$

$$Q_v = F_{dist} + F_{y2R} + F_{y2L} + (F_{x1R} + F_{x1L}) \sin(\delta) + (F_{y1R} + F_{y1L}) \cos(\delta) \quad (3.15b)$$

$$Q_r = F_{dist} \ell_{dist} + M_{yaw} + a \left((F_{x1R} + F_{x1L}) \sin(\delta) + (F_{y1R} + F_{y1L}) \cos(\delta) \right) - b(F_{y2R} + F_{y2L}) + \frac{w}{2} \left(F_{y2R} + (F_{x1R} - F_{x1L}) \cos(\delta) + (F_{y1L} - F_{y1R}) \sin(\delta) - F_{y2L} \right) \quad (3.15c)$$

$$Q_\varphi = - \left(a^2 \dot{\eta} (C_{1R} + C_{1L}) + b^2 \dot{\eta} (C_{2R} + C_{2L}) \right) \quad (3.15d)$$

$$Q_\eta = - \left(\frac{w^2}{4} \dot{\varphi} (C_{1R} + C_{2R}) + \frac{w^2}{4} \dot{\varphi} (C_{2L} + C_{1L}) \right) \quad (3.15e)$$

The forces that arises due to the dampers are derived using the same simplifications as the spring forces in the potential energy described previously, i.e. assuming small roll and pitch angles to obtain the velocities in the wheel hubs. C_{ij} in the equation are the damping coefficients of the dampers in the suspension system of the vehicle. Now, knowing the components of the Lagrangian, the generalised forces, and the composition of the equations of motion, the vehicles trajectory can be computed for the situation of interest.

3.2 From a four wheel model to a two wheel model

In the case of the four wheel vehicle model traveling in a circular path with a large turning radius, R , compared to the width of the vehicle, w , the four wheel vehicle model can be approximated as a two wheel model, i.e. a bicycle model. This assumption is valid due to the lateral symmetry of the vehicle and mostly due to the fact that the width is negligible compared to the turning radius, i.e. $w \ll R$.

Omitting the width of the vehicle eliminates the effects of lateral load transfer in the model, hence the φ -degree of freedom (vehicle roll) is eliminated from the analysis. To simplify the equations even further the height of the vehicle model is set to zero, $h = 0$. This yields that no longitudinal load transfer can occur due to the pitching motion of the vehicle, hence the η -degree of freedom is eliminated from the model, which gives that Equations 3.8d, 3.8e are omitted from the analysis. Without height and without the φ - and η -degrees of freedom the potential energy, V , of the system will be zero, thus $\bar{\mathcal{L}} = \bar{T}$. This gives the flat two wheel model shown in Figure 3.4.

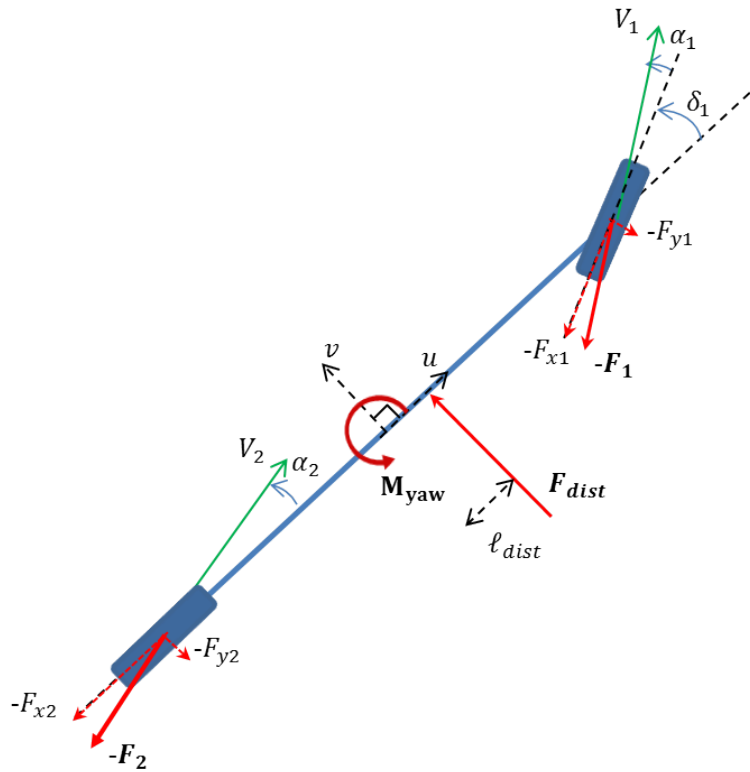


Figure 3.4: Schematic figure of 2-wheeled vehicle model

The quasi-coordinate motion equations remaining after the the aforesaid approximations and simplifications are shown below:

$$m(\dot{u} + rv) = F_{x1} \cos(\delta) - F_{y1} \sin(\delta) + F_{x2} \quad (3.16a)$$

$$m(\dot{v} - ru) = F_{x1} \sin(\delta) + F_{y1} \cos(\delta) + F_{y2} + F_{dist} \quad (3.16b)$$

$$I_{zz}\dot{r} = a(F_{x1} \sin(\delta) + F_{y1} \cos(\delta)) - bF_{y2} + M_{yaw} + F_{dist}l_{dist} \quad (3.16c)$$

Whether or not this system of equations is solvable is strongly dependent of the tyre model used to determine the lateral forces F_{yi} , on the complexity of the steering input δ , and on the simplicity of applied brake forces F_{xi} .

3.3 Derivation of the differential equation for the yaw velocity

To obtain an analytical model the equations of motion stated in Equation 3.16 is reduced to one single differential equation for the yaw velocity, $r(t)$. The reason for this reducing the system of motion equations down to an equation in the yaw velocity is that other motion parameters of interest can be computed once the expression for the yaw velocity is known. Therefore, solving the differential equation for the yaw velocity will be the key to determine the trajectory of the vehicle. From Equation 3.1 the yaw angle, $\Psi(t)$, is computed as shown below:

$$\Psi(t) = \int_0^t r(t)dt \quad (3.17)$$

With the yaw angle known the vehicle's global position is computed by integrating the inverse relation of Equation 3.1, as shown below:

$$X(t) = \int_0^t u(t) \cos(\Psi(t)) - v(t) \sin(\Psi(t)) dt \quad (3.18a)$$

$$Y(t) = \int_0^t u(t) \sin(\Psi(t)) + v(t) \cos(\Psi(t)) dt \quad (3.18b)$$

It is here that the requirement of analytical solvability comes in to play as the expressions obtained must be analytically integrable for the vehicle's trajectory to be computable without using numerical solvers.

The yaw velocity differential equation is obtained by reducing the equation system shown in Equation 3.16 together with the time derivative of Equation 3.16c down to one equation. Whereby the following differential equation for the yaw velocity is obtained:

$$f_0(u(t)) + f_1(u(t))r + f_2(u(t))r^2 + f_3(u(t))\dot{r} + f_4(u(t))r\dot{r} + f_5(u(t))r^2\dot{r} + f_6(u(t))r\dot{r}^2 + f_7(u(t))\ddot{r} = 0 \quad (3.19)$$

where the functions $f_0(u(t)) - f_7(u(t))$ are all long and complicated and strongly dependent of the velocity $u(t)$, i.e they are time-dependant. Due to the complexity of this differential equation, an analytical expression will not be possible to derive based on this expression. Therefore, the equation system 3.16 needs to be simplified for a analytically solvable differential equation to be derived from it.

3.3.1 Constitutive relations for the tyre slip angles

As mentioned previously, the solvability of the system of motion equations shown in Equation 3.16 is strongly dependant on how the lateral forces, F_{yi} , are modelled. As the lateral forces are dependant on the slip angles α_i , which are assumed to be small they can be approximated as linear functions of the slip angles, with the constant cornering stiffness $C_{F\alpha i}$ as shown in Equation 2.2. The slip angles are obtained from the constitutive relations derived from the schematic figure of the two-wheeled vehicle model shown in Figure 3.4 which with the assumption of small angles are expressed as:

$$\begin{aligned} \tan(\alpha_1 + \delta(t)) &\approx \alpha_1 + \delta(t) = \frac{v(t) + ar(t)}{u(t)} \\ \tan(\alpha_2) &\approx \alpha_2 = \frac{v(t) - br(t)}{u(t)} \end{aligned} \quad (3.20)$$

The steering angle, $\delta(t)$, is also assumed to be small resulting in a simplified form of the system of motion equations stated in Equation 3.16.

3.3.2 Linearisation of motion equations

By applying the methodology of linearisation explained in Section 2.3.2 to all of the time dependent parameters, except from the longitudinal velocity $u(t)$, the non-linear system of motion equations shown in Equation 3.16 can be written as a linear system. The linearized parameters are defined as illustrated below for the yaw velocity:

$$r(t) = r_0 + \tilde{r}(t) \quad (3.21)$$

The longitudinal velocity, $v(t)$, the slip angles, $\alpha_i(t)$ and the steer angle, $\delta(t)$ are all linearized in the same way. The parameters with zero subscripts are the constant components of the linearisation while the ones marked with tilde are the time dependant fluctuations, assumed to be small. The constant contributions are stated in the operating point in which the braking procedure is studied.

3.3.3 Operating point of interest

Since the analysis is performed for the case of a sudden severe braking situation while driving straight forwards some assumptions of the initial conditions and of the parameters governing the brake procedure can be made. As the car is driving straight forward it is reasonable to assume that the tyre slip-angles, α_i , the lateral velocity, v , the yaw angle Ψ , and the rotational velocity, r , are zero initially and small during the remaining part of the braking process. The steer angle, δ , is also zero initially but allowed to change during the procedure. The braking forces acting on the vehicle are assumed to be kept constant during the entire brake procedure. The assumptions made are expressed explicit in Equation 3.22.

$$\begin{aligned} \alpha_{i0} &= 0 & u(t) &= u_0 + a_x t \\ v_0 &= 0 & r_0 &= 0 \\ \delta_0 &= 0 & \psi_0 &= 0 \\ \tilde{v}(t) &\ll u(t) & \tilde{r}(t)\ell &\ll u(t) \\ F_{xi}(t) &= F_{xi} \quad (=Const) \end{aligned} \quad (3.22)$$

An assumption of less obvious nature is that the longitudinal velocity profile, $u(t)$, is linear, i.e. that the longitudinal acceleration is kept constant. This assumption is made to simplify the analytical calculations.

3.3.4 Reduction to a single differential equation

With the operating point defined as in the previous chapter together with the assumption that the product of two fluctuating terms (parameters labelled with tilde) approximately equals zero, the system of motion equations (Equation 3.16) is simplified. However, the system is still statically undetermined, therefore a fourth equation is needed. Assuming that the steering angle $\tilde{\delta}(t)$, defined as shown in Equation 2.6, is quasi static (see Section 2.1.5) with $\dot{v}(t)$ omitted for further simplicity, it is possible to differentiate the motion equation for the yaw velocity (Equation 3.16c) with respect to time without introducing any new parameters. This way the fourth equation needed for the system to solvable is obtained. The solvable system now looks like:

$$m\dot{u}(t) = F_{x1} + F_{x2} \quad (3.23a)$$

$$m\dot{\tilde{v}}(t) = \left(F_{x1} + C_{F\alpha1} \right) \tilde{\delta}(t) + F_{dist} - \frac{C_\alpha}{u(t)} \tilde{v}(t) - \left(\frac{C_\beta}{u(t)} + mu(t) \right) \tilde{r}(t) \quad (3.23b)$$

$$I_{zz}\dot{\tilde{r}}(t) = a \left(F_{x1} + C_{F\alpha1} \right) \tilde{\delta}(t) + M_{yaw} + F_{dist}\ell_{dist} - C_\beta \frac{\tilde{v}(t)}{u(t)} - C_\gamma \frac{\tilde{r}(t)}{u(t)} \quad (3.23c)$$

$$I_{zz}\ddot{\tilde{r}}(t) = \frac{\dot{u}(t)}{u(t)^2} \left(C_\beta \tilde{v}(t) + C_\gamma \tilde{r}(t) \right) - \frac{1}{u(t)} \left(C_\beta \dot{\tilde{v}}(t) + C_\gamma \dot{\tilde{r}}(t) \right) \quad (3.23d)$$

In Equation 3.23 three new constants are introduced, C_α , C_β and C_γ , defined as

$$\begin{cases} C_\alpha = C_{F\alpha 1} + C_{F\alpha 2} \\ C_\beta = aC_{F\alpha 1} - bC_{F\alpha 2} \\ C_\gamma = a^2C_{F\alpha 1} + b^2C_{F\alpha 2} \end{cases} \quad (3.24)$$

Equation 3.23 now contains a set of solvable equations and since the steering angle $\tilde{\delta}(t)$ is a function of the longitudinal velocity and the yaw velocity it is possible to reduce these equations down to one single differential equation in terms of the longitudinal velocity and derivatives of the yaw velocity. The tilde notation for the time dependent fluctuations will from this point on be dropped to simplify the expressions, however the reader should keep in mind that only the fluctuations of the yaw velocity are considered and that they are assumed small. The linearised differential equation for the yaw velocity takes the form:

$$D_0 u(t) + (D_{1a} + D_{1b} u(t)^2) r(t) + D_3 u(t) \dot{r}(t) + D_7 u(t)^2 \ddot{r}(t) = 0 \quad (3.25)$$

By the theory of Section 2.3.1 this differential equation is a nonautonomous, second order ordinary differential equation with time variant coefficients. Where the coefficients consists of one time variant factor, $u(t)$, and one constant factor, D_i , with the constant parts defined as follows:

$$\begin{cases} D_0 = m(C_\beta F_{dist} - (C_\alpha + F_x)(F_{dist} \ell_{dist} + M_{yaw})) \\ D_{1a} = m(C_\alpha C_\gamma - C_\beta^2) \\ D_{1b} = C_\beta m(\kappa_1(F_{x1} + C_{F\alpha 1}) - m) + C_\beta F_x(F_{x1} + C_{F\alpha 1}) \kappa_2 - am C_{F\alpha 1} (C_\alpha + F_x)(\kappa_1 + \kappa_2 \dot{u}(t)) \\ D_3 = m((C_\alpha + F_x) I_{zz} + C_\gamma m) \\ D_7 = m^2 I_{zz} \end{cases} \quad (3.26)$$

where F_x is the sum of the total braking force acting on the rear and on the front axle, i.e. $F_x = F_{x1} + F_{x2}$.

4 Combining two solution approaches to obtain the two wheel model

As seen in Chapter 3, all variables describing the vehicle motion (lateral velocity and acceleration, heading angle, global position, etc.) can be derived knowing the rotational velocity $r(t)$. Therefore, solving Equation 3.25 is the key when determining the motion of the vehicle. In this chapter the differential equation governing the rotational velocity is solved using different approaches and simplifications.

4.1 Vehicle parameters

The simulations and computations of this thesis study are done using vehicle parameters stated in the Licentiate thesis *On Drive Force Distribution and Road Vehicle Handling* by Matthijs Klomp, see Table 4.1 [11].

Table 4.1: Vehicle parameters

<i>Parameter</i>	<i>Value</i>	<i>Unit</i>	<i>Description</i>
a	1.4	[m]	Distance from CoM to front axle
b	1.6	[m]	Distance from CoM to rear axle
ℓ	3	[m]	Wheelbase
w	1.5	[m]	Track width
$C_{F\alpha_1}$	60 000	[N/rad]	Cornering stiffness front wheel
$C_{F\alpha_2}$	60 000	[N/rad]	Cornering stiffness front wheel
m	1 600	[kg]	Mass of vehicle
F_{z1}	8371	[N]	Static normal force at front wheel
F_{z2}	7325	[N]	Static normal force at front wheel
I_{zz}	2617	[kg m ²]	Moment of inertia for rotation about the z-axis
C_{L1}	0.136	[-]	Lift coefficient for vehicle front
C_{L2}	0.246	[-]	Lift coefficient for vehicle rear
A	2.17	[m ²]	Frontal area
h	0.5	[m]	Distance from ground plane to center of mass
ξ_{Tr}	0.005	[m]	Pneumatic trail
K_y	200 000	[N/m]	Lateral tyre stiffness
$\frac{\partial \delta}{\partial T_s}$	-0.0059	[rad/Nm]	Steering system compliance
μ	0.001	[-]	Friction coefficient dry asphalt

Parameters not mentioned above, such as the brake force F_x and the disturbances of the system, are varied during the study and are therefore not stated in the table. Which values that are used and how they are varied is mentioned in the context of each part of the study.

4.2 Combining Bessel- and constant velocity solutions yields the two wheel model

One of the milestones for the study is to find a simple expression that approximates the lateral drift during high speed braking of a vehicle. For this to be possible the differential equation for the yaw velocity, see Equation 3.25, must be solved analytically. Otherwise carrying out the integrations of Equation 3.18 will not be possible.

4.2.1 Time dependant coefficients in the differential equation

As the differential equation governing the yaw velocity, $r(t)$, derived in the previous chapter is nonhomogeneous its solution must consist of both a homogeneous and a particular solution to be unambiguously determined.

Homogeneous solution

The homogeneous solution to Equation 3.25 is obtained by solving the following differential equation:

$$(D_{1a} + D_{1b}u(t)^2)r(t) + D_3u(t)\dot{r}(t) + D_7u(t)^2\ddot{r}(t) = 0 \quad (4.1)$$

Comparing Equation 4.1 to the differential equation of Bessel shown in Equation 2.36 it is seen that they are similar in appearance except from the fact that $r(t)$ is not differentiated with respect to the velocity $u(t)$. By rewriting $r(t)$ such that it depends on the velocity $u(t)$ instead of the time, i.e such that $r = r(u(t))$, and by applying the chain rule on the derivatives, see Equation 4.2, Equation 3.25 is rewritten to fit the differential equation of Bessel (Equation 2.36).

$$\begin{cases} \frac{dr}{dt} = \frac{dr}{du(t)} \frac{du(t)}{dt} = a_x \frac{dr}{du(t)} \\ \frac{d^2r}{dt^2} = \frac{d}{dt} \left(\frac{dr}{du(t)} \right) = \frac{d}{dt} \left(a_x \frac{dr}{du(t)} \right) = a_x \frac{d}{du(t)} \left(\frac{dr}{du(t)} \right) = a_x^2 \frac{d^2r}{du(t)^2} \end{cases} \quad (4.2)$$

The differential equation for the yaw velocity $r(u(t))$ is now written as:

$$\frac{(D_{1a} + D_{1b}u(t)^2)}{D_7a_x^2}r(u(t)) + \frac{D_3}{D_7a_x}u(t) \frac{dr}{du(t)} + u(t)^2 \frac{d^2r}{du(t)^2} = 0 \quad (4.3)$$

Equation 4.3 is now identified as a differential equation of Bessel as shown in Equation 2.36, therefore its solution is known. This yields the homogeneous solution, $r_{B,hom}(t)$, as:

$$r_{B,hom}(t) = r(u(t)) = u(t)^{-\tilde{p}} \left[A_1 J_{\tilde{q}/\tilde{h}} \left(\frac{\tilde{\alpha}}{\tilde{r}} u(t)^{\tilde{h}} \right) + A_2 Y_{\tilde{q}/\tilde{h}} \left(\frac{\tilde{\alpha}}{\tilde{r}} u(t)^{\tilde{h}} \right) \right] \quad (4.4)$$

with the of the coefficients for the Bessel functions defined as:

$$\begin{aligned} \tilde{p} &= \frac{D_3 - D_7a_x}{2D_7a_x} & \tilde{\beta} &= \sqrt{\frac{D_{1a}}{D_7a_x^2}} \\ \tilde{q} &= \sqrt{\tilde{p}^2 - \tilde{\beta}^2} & \tilde{\alpha} &= \sqrt{\frac{D_{1b}}{D_7a_x^2}} \\ \tilde{h} &= 1 \end{aligned} \quad (4.5)$$

$r(t) = r_{B,hom}(t)$ now satisfies Equation 4.3, which the differential equation theory chapter of Section 2.3.4.1 corresponds to $y = r_{B,hom}(t)$ satisfying $F(t, r_{B,hom}(t), r'_{B,hom}(t), \dots) = 0$.

Particular solution

A particular solution to Equation 3.25 is complicated to find by using traditional methods as described in Section 2.3.4.3. However, it is known that after some time the behaviour of a solution of a differential equation is governed by its particular solution (given that the system is damped). Since the only types of disturbances analysed in this thesis are lateral force or yaw moment, each either acting as a constant disturbance or initial disturbance, and since the longitudinal velocity profile is assumed linear it can easily be deducted that the latter behaviour of the rotational velocity, $r(t)$, is governed by its first order terms and the velocity profile. Therefore it is at this point assumed that the first and second order time-derivative of the rotational velocity, together with their corresponding coefficients, are small compared to the other terms in the differential equation. This leads to that these terms can be omitted, leaving the first order terms of the yaw velocity. Which in turn leads to that the behavior of the latter part of the braking procedure is given by the expression shown in Equation 4.6. Since this expression is assumed to completely govern the latter part of the braking procedure it is taken as the particular solution:

$$r_{B,part}(t) = -\frac{D_0u(t)}{D_{1a} + D_{1b}u(t)^2} \quad (4.6)$$

The total solution of the rotational velocity for this case, with the velocity profile assumed as a linear function, is now obtained by adding Equations 4.4 and 4.6:

$$r_B(t) = r_{B,hom}(t) + r_{B,part}(t) = u(t)^{-\bar{p}} \left[A_1 \mathbf{J}_{\bar{q}/\bar{r}} \left(\frac{\tilde{\alpha}}{\bar{r}} u(t)^{\bar{r}} \right) + A_2 \mathbf{Y}_{\bar{q}/\bar{r}} \left(\frac{\tilde{\alpha}}{\bar{r}} u(t)^{\bar{r}} \right) \right] - \frac{D_0 u(t)}{D_{1a} + D_{1b} u(t)^2} \quad (4.7)$$

The coefficients A_1 and A_2 in Equation 4.7 are constants which are determined using initial conditions on $r_B(t)$. This solution will hereafter be referred to as the Bessel model.

Bessel functions are known to be tedious to integrate, especially if the coefficients of the Bessel functions are not integers, and therefore the Bessel solution alone fails to satisfy the goals of the study stated initially as it does not provide a rudimentary framework usable for further analysis of the system. An alternative, integrable model which mimics the Bessel model needs to be determined.

4.2.2 Constants coefficients in the differential equation

Following the work done by Professor Koiter and Professor Pacejka, it is assumed that the velocity $u(t)$ is constant, $u(t) = u_0$ [2]. Inserted into Equation 3.25 this yields that the coefficients D_0 , D_{1a} , D_{1b} , D_3 , and D_7 are reconstructed to simplify the differential equation to the following expression:

$$C_1 r(t) + C_3 \dot{r}(t) + C_7 \ddot{r}(t) = -C_0 \quad (4.8)$$

with the new coefficients defined as

$$\begin{cases} C_0 = m u_0 (C_\beta F_{dist} - (C_\alpha + F_x)(F_{dist} \ell_{dist} + M_{yaw})) \\ C_1 = (C_\alpha C_\gamma - C_\beta^2) m + u_0^2 \left(C_\beta F_x (C_{F\alpha 1} + F_{x1}) \kappa_2 - a C_{F\alpha 1} (C_\alpha + F_x) (\kappa_1 + a_x \kappa_2) m + \right. \\ \quad \left. C_\beta m ((C_{F\alpha 1} + F_{x1}) \kappa_1 - m) \right) \\ C_3 = m u_0 ((C_\alpha + F_x) I_{zz} + C_\gamma m) \\ C_7 = u_0^2 m^2 I_{zz} \end{cases} \quad (4.9)$$

This differential equation, Equation 4.8, is solvable using the method shown in Section 2.3.4.1, as it is a second order, non-homogenous ordinary differential equation with constant coefficients and it is therefore solved using traditional methods.

Homogeneous solution

The homogeneous part of the solution of Equation 4.8 is found by solving the following differential equation, using the theory of described in Section 2.3.4:

$$C_1 r(t) + C_3 \dot{r}(t) + C_7 \ddot{r}(t) = 0 \quad (4.10)$$

The characteristic equation corresponding to this differential equation becomes:

$$\frac{C_1}{C_7} + \frac{C_3}{C_7} \lambda + \lambda^2 = 0 \quad (4.11)$$

And the roots of this equation becomes:

$$\lambda_{1,2} = -\frac{C_3}{2C_7} \pm \sqrt{\left(\frac{C_3}{2C_7}\right)^2 - \frac{C_1}{2C_7}} \quad (4.12)$$

Which then yields the homogeneous solution for the rotational velocity as:

$$r_{CV,hom}(t) = A_1 e^{\lambda_1 t} + A_2 e^{\lambda_2 t} \quad (4.13)$$

Particular solution

Since the right hand side of differential equation of Equation 4.8, i.e. $-C_0$, is constant the particular solution will also be constant. It is therefore assumed that $r_{part}(t) = A_3$, which inserted into Equation 4.8 results in following expression:

$$C_1 A_3 = -C_0 \quad (4.14)$$

Resulting in that the particular solution becomes:

$$r_{CV,part}(t) = -\frac{C_0}{C_1} \quad (4.15)$$

The complete solution for the rotational velocity for this simplified case therefore becomes:

$$r_{CV}(t) = r_{CV,hom}(t) + r_{CV,part}(t) = A_1 e^{\lambda_1 t} + A_2 e^{\lambda_2 t} - \frac{C_0}{C_1} \quad (4.16)$$

where the constants A_1 and A_2 are obtained by using initial conditions for $r(t)$. This solution will hereafter be referred to as the Constant velocity model. Studying the article *Skidding of vehicles due to locked wheels* [2] it is seen that without any continuous disturbances of the system, the Constant velocity model resembles the Bessel model (Equation 4.7). However, in the case with a continuous disturbance in the system only the initial phases for the models will correlate as the Constant velocity model will converge to a non-zero value due to the constant term in the differential equation (see Equation 4.8), whereas the Bessel model will give zero rotational velocity at stand still. Even though this Constant velocity model is integrable, it needs to be improved.

4.2.3 Analytical solution to the two wheel model

Since the Constant velocity model captures the behaviour of the Bessel model at the initial phase but not at the end, it seems that there is need for a different particular solution in the Constant velocity model. As the particular solution used in the Bessel model completely governs the behaviour at the end, it should be a valid particular solution even for the integrable analytical model. The new model is therefore expressed as:

$$r(t) = r_{hom}(t) + r_{part}(t) = r_{CV,hom}(t) + r_{B,part}(t) = A_1 e^{\lambda_1 t} + A_2 e^{\lambda_2 t} - \frac{D_0 u(t)}{D_{1a} + D_{1b} u(t)^2} \quad (4.17)$$

Since this expression for the vehicle's rotational velocity is built upon two relatively simple models it is possible to integrate this function to obtain the heading angle Ψ . This model will hereafter be referred to as the analytical two wheel model.

4.2.4 Derivation of initial conditions

The initial conditions are needed to find an unambiguous solution to the equations governing the rotational velocity (Equation 4.17), i.e. to determine the constants A_1 and A_2 . To find the relations between the disturbances and the initial conditions it is assumed that an impulse moment is acting on a arbitrary point on the car for an infinitesimally short period of time. In this short period it is assumed that the vehicle is driving straight forward with zero rotation and no wheel slip.

The initial condition for rotational velocity at time zero is derived from the rotational velocity motion equation stated in Equation 3.16c. As only the initial stage is considered both the slip angles and the steering angle will be zero, therefore only the disturbances remain in the right hand side of the equation. Since only moment disturbances are considered in the analysis the disturbance force F_{dist} are set to zero reducing the yaw velocity motion equation to the following expression;

$$I_{zz} \frac{dr}{dt} = M_{yaw} \quad (4.18)$$

By solving these equations as separable differential equations the initial conditions is obtained:

$$\int_0^{r_0} I_{zz} dr = \int_{0^-}^{0^+} M_{yaw} dt \quad (4.19)$$

For the moment disturbance to be active only when $t = 0$ the disturbance is modeled as a moment impulse, \mathcal{M}_{yaw} , as shown in Equation 4.20. Note that as \mathcal{M}_{yaw} is a moment impulse its unit are $Nm \cdot s$.

$$M_{yaw} = \mathcal{M}_{yaw} \delta_D(t) \quad (4.20)$$

Where $\delta_D(t)$ is the Dirac delta function which causes the disturbance to be active only at $t = 0$. Inserting Equation 4.20 into Equation 4.19 and carrying out the integrations gives the initial conditions as:

$$r_0 = \frac{\mathcal{M}_{yaw}}{I_{zz}} \quad (4.21)$$

For the case of the initial disturbance being a force F_{dist} , and not a moment M_{yaw} , the product \mathcal{M}_{yaw} is simply replaced by $\mathcal{P}_{dist} \ell_{dist}$, \mathcal{P} is an impulse force. The second initial condition needed to determine an unambiguous solution for $r(t)$ is that of $\dot{r}(0) = \dot{r}_0$, which is obtained from Equation 3.23c by putting $t = 0$. This way eliminating the lateral velocity and the steer angle from the expression. The second initial condition then becomes as follows:

$$\dot{r}_0 = \frac{1}{I_{zz}} \left(M_{yaw} - C_\gamma \frac{r_0}{u_0} \right) \quad (4.22)$$

Whereby the constants A_i can now be determined.

4.2.5 Comparing results of differential equation solution procedures

The Bessel model, the Constant velocity model and the analytical two wheel model are compared in Figure 4.1 below to verify that the analytical two wheel model is a good approximation for the yaw velocity.

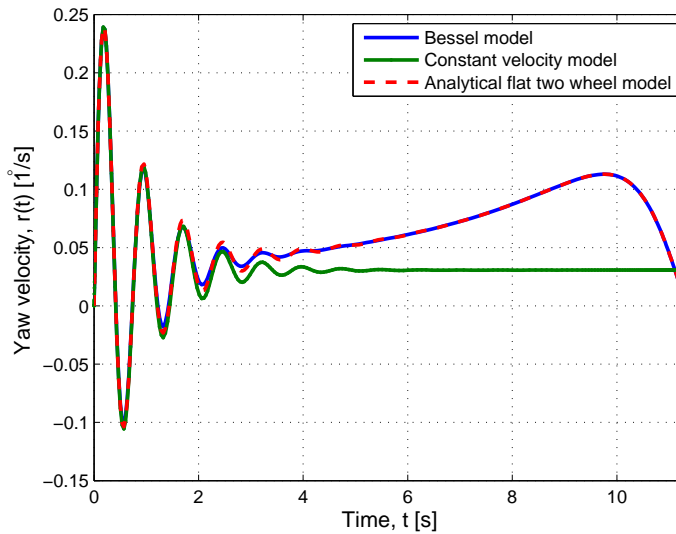


Figure 4.1: Comparison of the rotational velocity, $r(t)$, computed using the different models with the disturbance $M_{yaw} = 100Nm$ and the brake force $F_x = 0.6mg$

The figure shows the yaw velocity, $r(t)$, as the vehicle brakes from 240 km/h to standstill, computed using the three different solution approaches. As seen in the figure the analytical two wheel model is a fairly good approximation of the Bessel model and the expression is analytically integrable.

To further confirm the validity of the analytical model, the case of an initial impulse disturbance is studied and the result obtained from the Bessel model, the Constant velocity model and the analytical two wheel model are compared, see Figure 4.2.

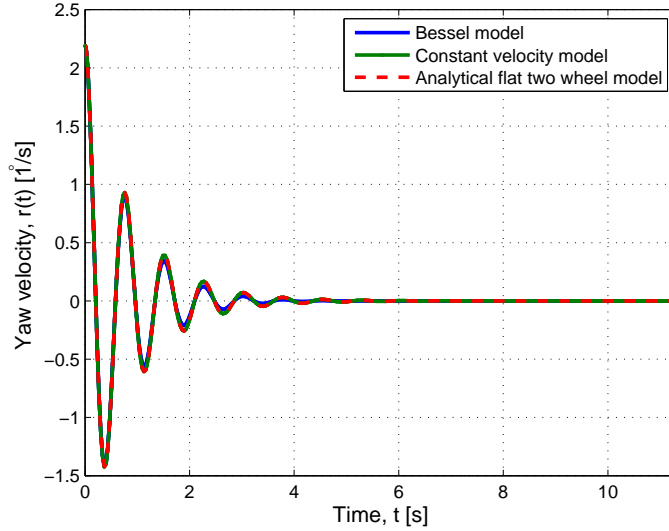


Figure 4.2: Comparison of the rotational velocity, $r(t)$, computed using different approaches with an initial impulse disturbance of $F_{dist} = 100 \text{ Nms}$ and the brake force $F_x = 0.6mg$

The figure shows that all three models give identical results, which is expected since this is equivalent to comparing the homogenous solutions of the previous analysis. In other words, equivalent to only comparing the initial part of the behaviour of the constant moment disturbance analysis shown in Figure 4.1.

4.3 Validation of the two wheel model

To validate the simple flat two wheel model derived in Section 4.2.3 the results from this model is compared to numerical solutions of the less simplified four wheel model derived in Section 3.1.

4.3.1 Solving the equations of motion for the four wheel model

To solve compute the motion for the four wheel model the equations of motion shown in Equation 3.8 must be solved. The generalized forces, Q_i , which constitute the right hand side of the equation system are given by Equation 3.15. The kinetic energy, \bar{T} , and the potential energy, V , are given by Equations 3.9 and 3.14 respectively. Linearized around the operating point and assuming small roll and pitch angles gives the left hand side of the equation system as shown below:

$$\frac{d}{dt} \left(\frac{\partial \bar{\mathcal{L}}}{\partial u} \right) - r \frac{\partial \bar{\mathcal{L}}}{\partial v} = hm\ddot{\eta}(t) + m\dot{u}(t) \quad (4.23a)$$

$$\frac{d}{dt} \left(\frac{\partial \bar{\mathcal{L}}}{\partial v} \right) + r \frac{\partial \bar{\mathcal{L}}}{\partial u} = m(\dot{v}(t) - h\ddot{\varphi}(t) + r(t)u(t)) \quad (4.23b)$$

$$\frac{d}{dt} \left(\frac{\partial \bar{\mathcal{L}}}{\partial r} \right) - v \frac{\partial \bar{\mathcal{L}}}{\partial u} + u \frac{\partial \bar{\mathcal{L}}}{\partial v} = I_{zz}\dot{r}(t) + I_{yz}\ddot{\eta}(t) + I_{xz}\ddot{\varphi}(t) - 2hm\dot{\varphi}(t)u(t) - hm\dot{u}(t)\varphi(t) \quad (4.23c)$$

$$\begin{aligned} \frac{d}{dt} \left(\frac{\partial \bar{\mathcal{L}}}{\partial \dot{\varphi}} \right) - \frac{\partial \bar{\mathcal{L}}}{\partial \varphi} = & w^2\varphi(t) \frac{1}{4} (K_{1L} + K_{2L} + K_{1R} + K_{2R}) + w\eta(t) \frac{1}{2} (a(K_{1R} - K_{1L}) + \\ & b(K_{2L} - K_{2R})) + I_{xy}\ddot{\eta}(t) + I_{xz}\dot{r}(t) + I_{xx}\ddot{\varphi}(t) + \\ & mh(h\ddot{\varphi}(t) + u(t)r(t) - \dot{v}(t)) \end{aligned} \quad (4.23d)$$

$$\begin{aligned} \frac{d}{dt} \left(\frac{\partial \bar{\mathcal{L}}}{\partial \dot{\eta}} \right) - \frac{\partial \bar{\mathcal{L}}}{\partial \eta} = & \eta(t) (a^2(K_{1L} + K_{1R}) + b^2(K_{2L} + K_{2R})) + w\varphi(t) \frac{1}{2} (a(K_{1R} - K_{1L}) + \\ & b(K_{2L} - K_{2R})) + I_{yz}\dot{r}(t) + I_{yy}\ddot{\eta}(t) + I_{xy}\ddot{\varphi}(t) + \\ & mh(\dot{u}(t) + h\ddot{\eta}(t) - g\eta(t)) \end{aligned} \quad (4.23e)$$

whereby the motion equations of the four wheel model are fully known.

4.3.2 Comparison of the two and four wheel model

The flat two wheel model derived in Section 4.2.3 is in this part of the analysis compared to the solution of Lagrange's equations of motion for the four wheel model. The equations governing the motion of the four wheel model is solved numerically using Matlab's differential equation solver *ode45.m*. The figure below shows the rotational velocity, $r(t)$, from both the analytical flat two wheel model and the numerical results from the four wheel model.

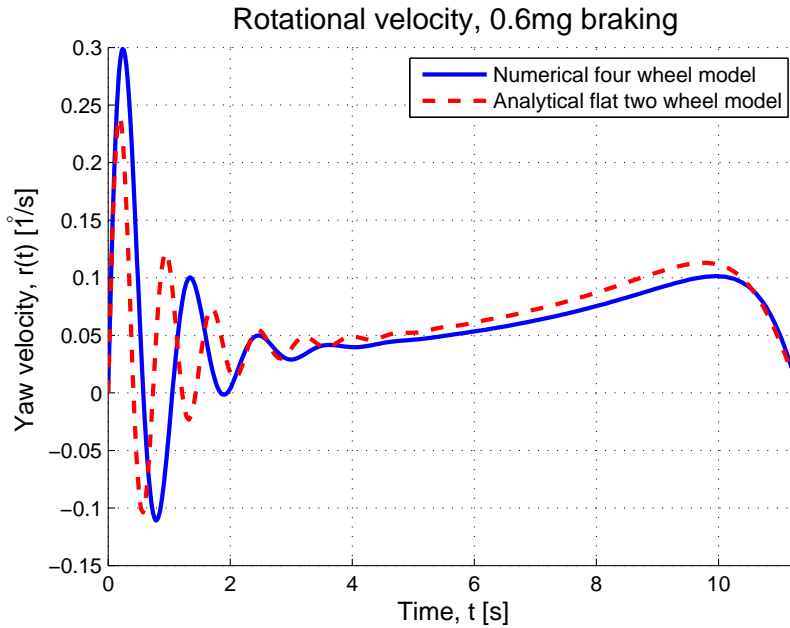


Figure 4.3: Comparison of the rotational velocity, $r(t)$, from the analytical two wheel model and the numerically solved four wheel model at a severe braking from $u_0 = 240$ km/h to stand still, with the disturbance $M_{yaw} = 100$ Nm and the brake force $F_x = 0.6mg$

As seen in the figure the analytical model is more oscillating and less damped than the numerical model. It is however still seen as a good approximation since the general behaviour is captured and the models are close to coincide a couple of seconds into the procedure. The small difference between the models is proved to be of less significance since the yaw velocity is integrated two times to obtain the lateral drift and with each integration, the difference between the models becomes less eminent.

The lateral drift is calculated for both models using Equation 3.18, where the yaw angle, $\Psi(t)$, is obtained by integrating the yaw velocity. Equation 3.18 however needs to be simplified by assuming that the yaw angle is small to obtain an analytical expression for the lateral drift. The analytical expression for the lateral drift is therefore defined as:

$$Y(t) = \int_0^t u(t)\Psi(t) + v(t)dt \quad (4.24)$$

The lateral drift for both models are presented in the figure below.

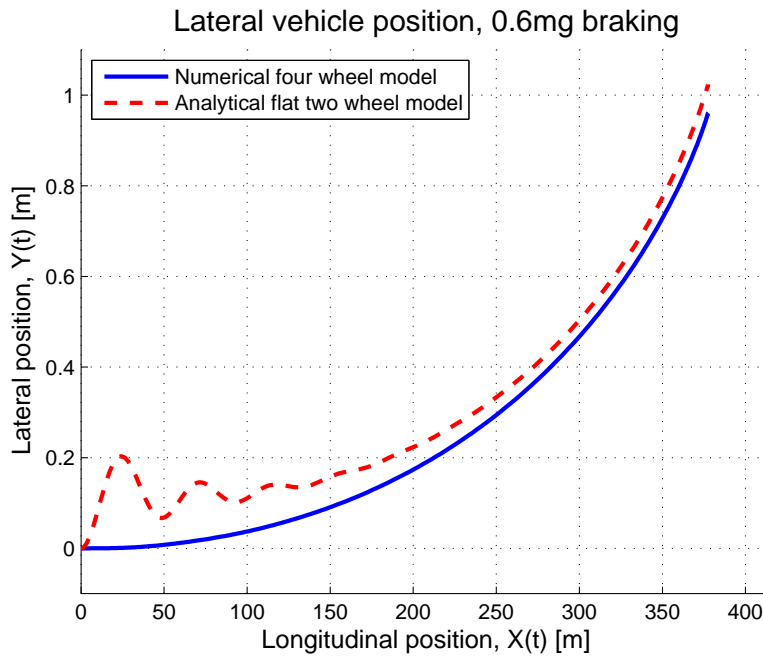


Figure 4.4: Comparison of the rotational lateral drift, $Y(t)$, from the analytical two wheel model and the numerically solved four wheel model at a severe braking from $u_0 = 240 \text{ km/h}$ to stand still, with the disturbance $M_{yaw} = 100 \text{ Nm}$ and the brake force $F_x = 0.6mg$

The figure shows that the biggest difference between the models occurs at the beginning. It can also be seen that the same tendencies of a less damped analytical model occurs in the lateral drift as well. However, after a couple of seconds the models start to coincide, which gives that the final value of the lateral drift for both models are very close.

5 Model analysis

To analyse the need of inherent vehicle stability during braking at high speed with disturbances of the system and to help motivate the importance of the study a frequency analysis of the model is carried out, more precisely an eigenfrequency and a frequency response analysis. The vehicle's yaw rate, i.e. rotational velocity, and lateral acceleration response to the steer angle δ is what the analysis focuses on. The effects of including more sophisticated tyre models, load transfer, and lateral force steer is analysed in this chapter as well. This is to help identify significant parameters from a stability point of view.

5.1 Frequency analysis

The stability of the two wheel model is evaluated in a frequency response analysis, to examine how the vehicle's response to steer angle input changes as the velocity is decreased. Further information about the vehicle's inherent stability is obtained by performing an eigenfrequency analysis.

5.1.1 Eigenfrequency

In order to determine the eigenfrequency of the model the differential equation in $r(t)$ shown in Equation 3.25 is rewritten to coincide with the standard form differential equation used in frequency analysis, shown in Equation 2.27, to obtain the following equation.

$$\ddot{r}(t) + \frac{D_3 u(t)}{D_7 u(t)^2} \cdot \dot{r}(t) + \frac{(D_{1a} + D_{1b} u(t)^2)}{D_7 u(t)^2} \cdot r(t) = -\frac{D_0 u(t)}{D_7 u(t)^2} \quad (5.1)$$

Termwise identification with the terms of Equation 2.27 yields the following expressions for the eigenfrequency and the damping factor:

$$\begin{cases} \omega = \sqrt{\frac{D_{1a} + D_{1b} u(t)^2}{u(t)^2 D_7}} \\ \xi = \frac{1}{2\omega} \cdot \frac{D_3}{u(t) D_7} \end{cases} \quad (5.2)$$

with the constants D_i shown in Equation 3.26. The eigenmodes of the model is determined by computing the roots to the characteristic equation of the expression shown in Equation 5.1:

$$\lambda^2 + 2\xi\omega\lambda + \omega^2 = 0 \Rightarrow \lambda_{1,2} = \omega(-\xi \pm \sqrt{\xi^2 - 1}) \quad (5.3)$$

As seen in Equation 3.26 the differential equation coefficients D_i include the braking forces, F_{xi} and the disturbances M_{yaw} and F_{dist} which all are external forces applied to the system. Therefore, for the natural eigenfrequency of the model to be obtained these need to be set to zero. If this is carried out the following expressions is obtained:

$$\omega = \sqrt{\frac{-C_\beta^2 m + C_\alpha C_\gamma m + (a(\kappa_1 + a_x \kappa_2) C_\alpha C_{F\alpha 1} + m C_\beta (\kappa_1 C_{F\alpha 1} - m)) u^2}{I_{zz} m^2 u^2}} \quad (5.4)$$

$$\xi = \frac{C_\alpha I_{zz} + C_\gamma m}{2 I_{zz} m \omega u}$$

Using the parameter values stated in Section 4.1 the eigenfrequency and damping is plotted for $u(t) = 240$ km/h to $u(t) = 120$ km/h, see Figure 5.1.

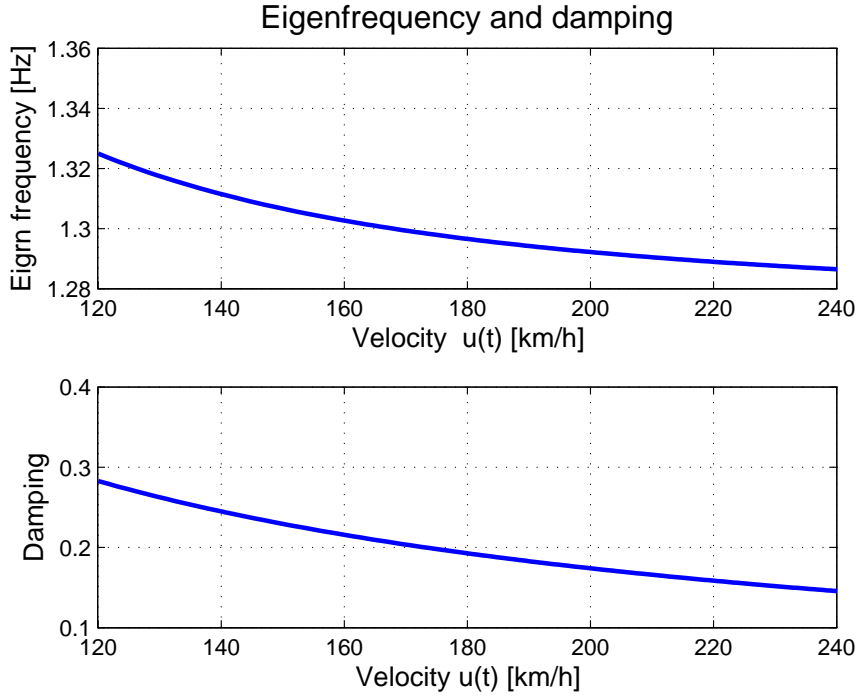


Figure 5.1: *Eigenfrequency and damping of the vehicle as the velocity is decreased from 240 to 120 km/h*

The figure shows how both the eigenfrequency and the damping are low for $u(t) = 240$ km/h and how these properties increase as the velocity decreases, i.e. how the stability of the vehicle increases as velocity decreases. The stability of the vehicle is increased during the deceleration as low eigenfrequency and damping are more dangerous as the uncontrollable oscillations occur at regions close to those in which the driver operates the vehicle, for example by steering angle input.

It should be clarified that for the results shown in Figure 5.1 to be valid the velocity decrease must be moderate. For hard braking the dynamics of the braking procedure will influence both the eigenfrequency and damping. Therefore, the purpose of the plots are mainly for comparison of the eigenfrequency at the initial and final velocity.

5.1.2 Frequency response

In this section the frequency response from the driver steer angle input to the yaw rate and the lateral acceleration is determined. The analyse are done both for the initial velocity $u_0 = 240$ km/h and the final velocity $u_1 = 120$ km/h.

The equation system shown in Equation 3.16 is linearised around the operating point described in Section 3.3.3 and with the velocity profile of $u(t)$ replaced by the constant velocity u_0 , and for the second analysis u_1 . The disturbances, M_{yaw} and F_{dist} , and braking forces, F_{xi} , are set to zero and the linear tyre model shown in Equation 2.2 is employed. The remaining equations are now rewritten in a state-space representation according to Section 2.3.3 to obtain the following equation system with the steer angle δ as only input.

$$\dot{\mathbf{x}} = \mathbf{A}\mathbf{x} + \mathbf{B}u \quad (5.5)$$

With the system matrix, \mathbf{A} , and input matrix, \mathbf{B} , as shown below

$$\mathbf{A} = \begin{bmatrix} \frac{C_\alpha}{mu_0} & -u_0 - \frac{C_\alpha}{mu_0} \\ -C_\beta & -C_\gamma \\ \frac{I_{zz}u_0}{I_{zz}u_0} & \frac{I_{zz}u_0}{I_{zz}u_0} \end{bmatrix} \quad \mathbf{B} = \begin{bmatrix} \frac{C_{F\alpha 1}}{m} \\ aC_{F\alpha 1} \\ I_{zz} \end{bmatrix} \quad (5.6)$$

and then matrices \mathbf{x} and \mathbf{u} as

$$\mathbf{x} = \begin{bmatrix} v \\ r \end{bmatrix} \quad u = \delta \quad (5.7)$$

To determine the frequency response the output of the system, \mathbf{y} , must be defined and formulated in state-space form, which is done in Equation 5.8 and Equation 5.9 respectively.

$$\mathbf{y} = \begin{bmatrix} a_y \\ r \end{bmatrix} = \begin{bmatrix} \dot{v} + u \cdot r \\ r \end{bmatrix} \quad (5.8)$$

$$\mathbf{y} = \mathbf{C}\mathbf{x} + \mathbf{D}u \quad (5.9)$$

The matrices \mathbf{C} and \mathbf{D} of Equation 5.9 are the output and feedthrough matrices shown in detail in Equation 5.10.

$$\mathbf{C} = \begin{bmatrix} -C_\alpha & -C_\alpha \\ \frac{mu_0}{0} & \frac{mu_0}{1} \end{bmatrix} \quad \mathbf{D} = \begin{bmatrix} C_{F\alpha 1} \\ m \\ 0 \end{bmatrix} \quad (5.10)$$

The frequency response of the matrix formulated equation system of Equation 5.5 and 5.9 is computed by use of Matlab's control system toolbox. The goal of the analysis is to compute the gain in the vehicle's yaw rate and lateral acceleration for different frequencies of the steer angle input, i.e. how different steer angle input frequencies are amplified in the yaw rate (yaw velocity) and lateral acceleration. Which gives an indication of the driver's controllability of the vehicle by use of the steer angle input. Figure 5.2 and 5.3 illustrates the result of the analysis when the system is linearised around the operating point (see Section 3.3.3) with $u_0 = 240$ km/h and around the point at which the vehicle has reached the desired velocity $u_1 = 120$ km/h.

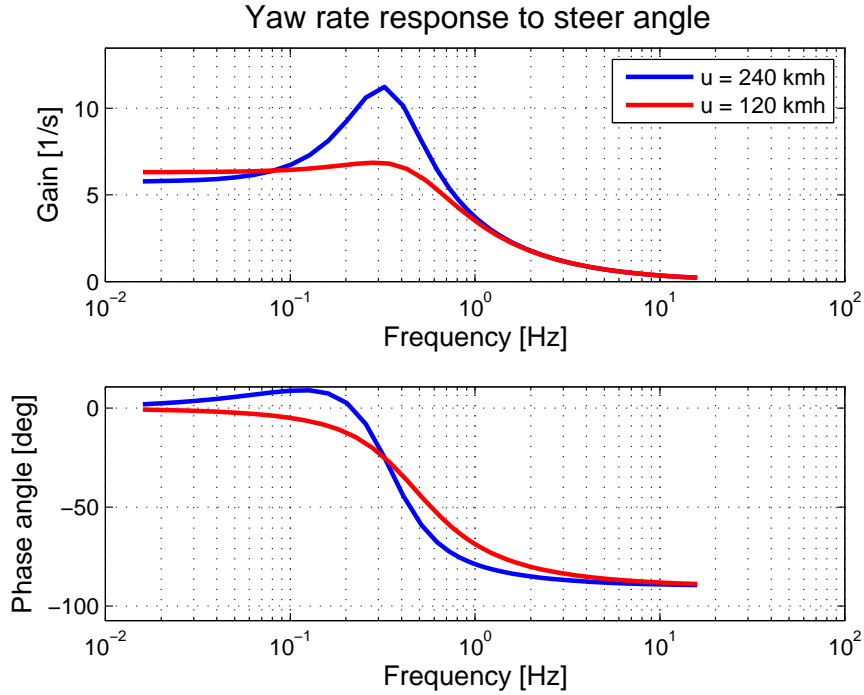


Figure 5.2: Yaw rate response to steer angle input

Lateral acceleration (normalized w.r.t. g) response to steer angle

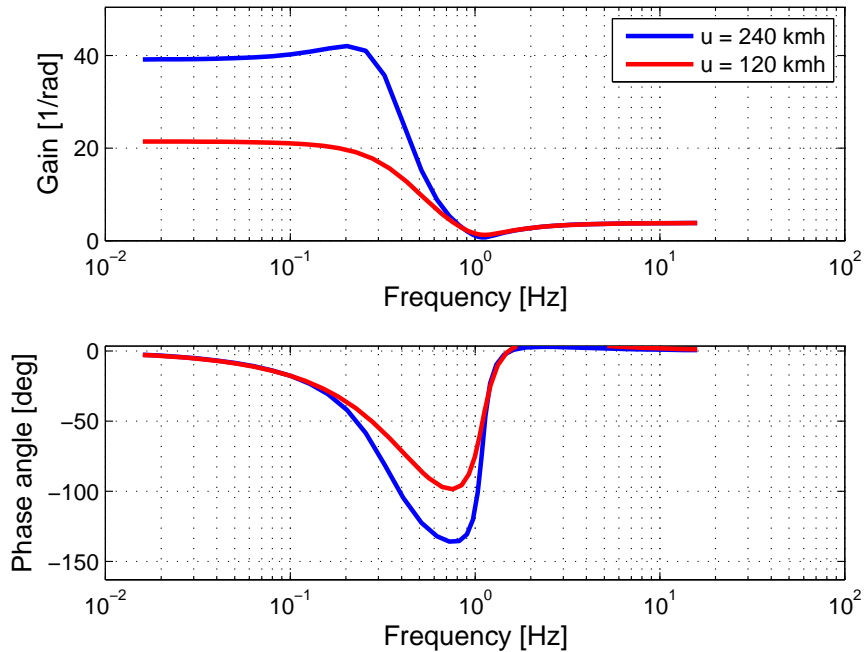


Figure 5.3: *Lateral acceleration response to steer angle input*

As seen in both Figure 5.2 and 5.3, the gain in yaw rate, $r(t)$, and lateral acceleration, $a_y(t)$, is very high for velocities of the magnitude $u_0 = 240$ km/h with steer angle input frequencies around those normal for operating a vehicle. At half of the initial velocity the gain in yaw rate and lateral acceleration is much less, which is a strong indicator of the importance of the vehicles inherent stability at high velocities. This since the driver's steer angle input at the initial velocity has dramatic influence on the vehicle dynamics which makes operating the vehicle both difficult and dangerous. However, at the velocity $u_1 = 120$ km/h the gains are of less dramatic proportions making the vehicle more controllable. This is not only an indicator of the importance of inherent vehicle stability, but also of the severity of the situation when braking hard at high speed.

5.2 Stability analysis

In optimization of the chassis parameters of a vehicle there are several criteria which needs to be met, for example the vehicle must be stable, be comfortable, be economic, be easily controlled, be safe in case of a crash, etc. These criteria and limitations give rise to optimisation contradictions, therefore the optimal set of parameters is a compromise of the desirable characteristics mentioned previously [3].

5.2.1 Multiple limits of stability, safety, and comfortability

The stability concept of this analysis follows the definition prescribed in Section 2.4. Therefore all vehicle parameters of the model affects the stability, however in this analysis all parameters except the cornering stiffness $C_{F\alpha 1}$ and $C_{F\alpha 2}$ are kept constant. The reason for this is that these are the most governing for the stability and also that they are relatively easy to control by choice of wheel settings and tyre properties.

For the reason of making comparisons with the technical report paper [3] easier and to simplify the implementation of different stability limits the cornering stiffness parameters $C_{F\alpha 1}$ and $C_{F\alpha 2}$ are replaced by the expressions shown in Equation 5.11 [3].

$$C_{F\alpha 1} = \frac{mb}{D_f \ell} \quad C_{F\alpha 2} = \frac{ma}{D_r \ell} \quad (5.11)$$

This gives that the variable parameters in the analysis now are the cornering compliances for the front and rear axles, D_f and D_r . The approximative model derived in Section 4.2.3 is now used to evaluate which combinations of these parameters that satisfies the conditions for stability.

The first and most trivial stability condition is the lateral drift during the braking procedure, see Equation 5.12

$$Y(t)|_{u(t)=u_1} < Y_{lim} \quad (5.12)$$

where Y_{lim} is typically half the width of a highway lane and u_1 the velocity at which the driver is assumed to be able to steer the vehicle within the lane without losing control. This limitation is trivial in the sense that if it is exceeded the vehicle will have drifted out of its lane and possibly off the road or onto the wrong side of the road.

The next limit for the stability condition is of less trivial nature, namely the limitation in the peak value for the rotational velocity, $r(t)$, shown in Equation 5.13.

$$\max(r(t))|_{t < 1s} < r_{lim} \quad (5.13)$$

The limit r_{lim} is set to keep the experience pleasant for the driver during the braking procedure. As mentioned in Section 5.12, if the initial peak for this parameter is too high the driver might react with violent movements of the steering wheel which most likely will cause the vehicle to lose control. This limit is completely subjective and therefore hard to determine as they are completely dependent of the driver's experience of similar situations. Again, as mentioned previously, documented experiences of professional test drivers will be used as guidelines when determining the limit r_{lim} .

Another condition that the model should fulfill for it to be seen as stable is that the vehicle's yaw velocity response frequency to the driver's steering input must be low for the driver to be able to steer the vehicle in a controlled fashion in an avoidance manoeuvre. For this to be feasible the eigenfrequency of the vehicle must not be located at the same low frequency as the yaw velocity response frequency. Therefore there is a lower limit to the vehicle's eigenfrequency, shown in Equation 5.14 [3].

$$\omega > \omega_{lim} \quad (5.14)$$

Here ω is the eigenfrequency given by Equation 5.2. If the eigenfrequency would be lower than ω_{lim} then the driver's steer input frequency could be in a frequency span close to the eigenfrequency which would give a violent increase in the yaw velocity response. This would give inconsistent vehicle behaviour as the yaw velocity response would be much stronger for certain steer input frequencies. This is the complete opposite of safe vehicle behaviour as consistent behaviour in all driving situations is the key factor in driving safety [3].

For the vehicle to have stable operating characteristics at the velocities considered in this study it is not allowed to be oversteered. This gives that combinations of the front and rear axle compliances D_f and D_r that gives negative understeer coefficients are not allowed, which gives the understeer coefficient (see Equation 2.5) as:

$$\varepsilon > 0 \quad (5.15)$$

The reason that oversteered vehicle characteristics are of no interest in this study is that this behaviour is uncontrollable at the velocities considered and will therefore give instability. As mentioned in Section 2.1.1, this phenomena occurs when the effective cornering stiffness of the front axle is greater than that of the rear axle. Analysing Equations 5.11 and 2.5 gives that the inequality of Equation 5.15 is satisfied for $D_f > D_r$. [15]

The model allows two types of disturbances; a moment about the z -axis and a point force acting in the direction of the y -axis. The influence of these disturbances on the system may be analysed both individually or as combined disturbances. They may also be used as initial disturbances, continuous throughout the braking procedure or as a combination of these two. Physical interpretations of these disturbances can be seen as a wind gust acting in the lateral direction resulting in a point force and an uneven distribution of brake force between the right and left wheels resulting in a moment around the z -axis. The moment disturbance can also be seen as an lateral offset of the vehicle's center of mass (CoM). However, only a constant moment about the z -axis acting continuously throughout the braking procedure is studied in this thesis.

5.2.2 Compromise of the desirable characteristics

Using the expressions of Equation 5.11 all limits and conditions stated in Section 5.2.1 can be expressed in terms of the effective cornering compliances D_f and D_r . This enables the limits to be plotted in the same figure to help illustrate the optimal compromise of the desirable characteristics. Using the model described in Section 4.2.3 and the cornering compliances the limits are plotted for the case the braking force $0.4mg$ being distributed 60% on the front wheel and 40% on the rear, see Figure 5.4. The numeric values for the limits used are shown Table 5.1 below.

Table 5.1: Numeric values for stability limits

Limit parameter	Numeric value	Unit
Y_{lim}	1, 2	[m]
r_{lim}	1	[1° /s]
$\omega_{n,lim}$	5	[rad/s]

All numeric values, except Y_{lim} , are taken from the technical report paper *Combining Properties of Driving Pleasure and Driving Safety: A Challenge for the Chassis Engineer* written by Johan Wedlin *et.al* [3]. The lateral drift limit Y_{lim} is set to one and two meters since this is the approximate span of the drift limit to keep the vehicle within it's lane during the braking procedure.

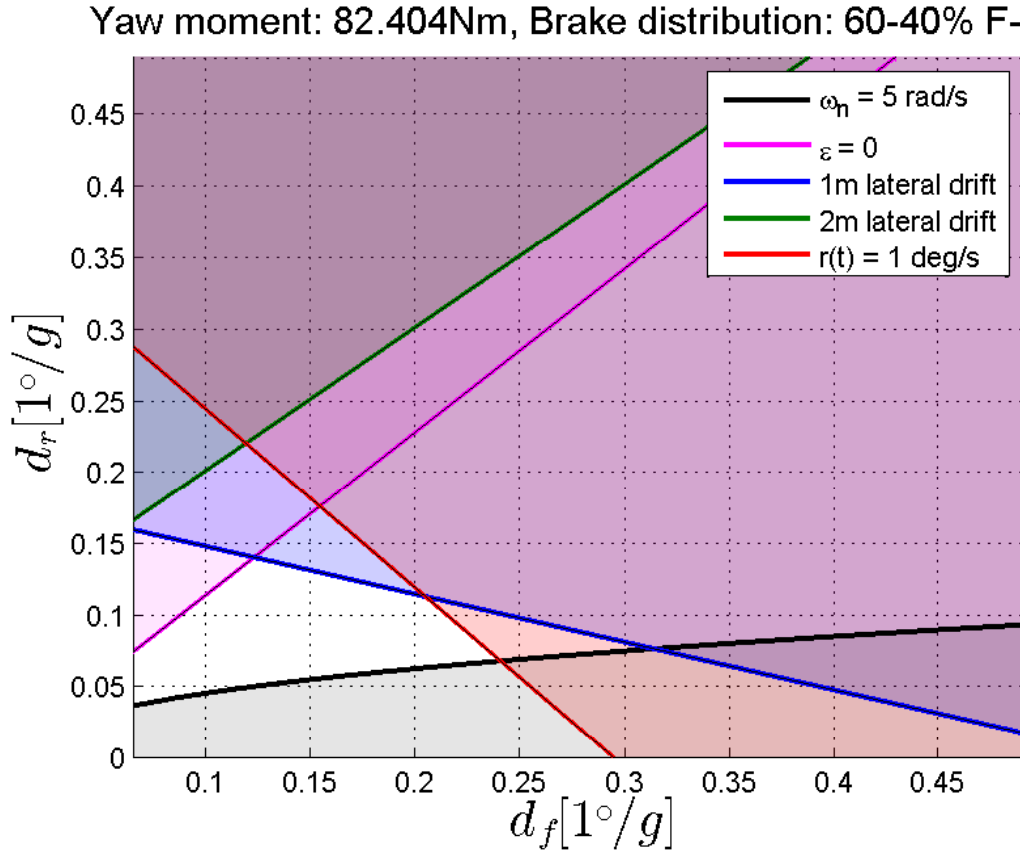


Figure 5.4: Stability limits plotted as functions of the cornering compliances

The shaded areas in the figure represents the combinations of the front and rear cornering compliances that does not fulfill one, or more, of the stated conditions. The un-shaded area represent the combinations that does fulfill all conditions and therefore are candidates for a fair compromise of the desired vehicle characteristics. The parameters shown on the axis are d_f and d_r , which is the cornering compliances D_f and D_r normalized by the gravity constant g . Therefore the physical interpretation of the compliance is degrees of slip angle per lateral acceleration. As seen in the figure all of the limits stated in Table 5.1 acts as limits for the stable pairs

of front and rear compliance, i.e. each of the limits constitutes a specific part of boundaries to the unshaded area in the plot.

The disturbance used in this stability analysis is the resulting moment from the drivers mass, $m_d = 70 \text{ kg}$, with a 20 cm lateral offset from the vehicle's longitudinal symmetry plane at $0.4mg$ brake force. Just as in previous analyses, the braking procedure analysed is when the vehicle decelerates from 240 km/h down to 120 km/h .

To see the effect of the brake distribution during the braking procedure the tyre model that takes into account combined slip (see Equation 2.3) is used in the compliance analysis. The brake distribution is varied by changing the brake forces F_{x1} and F_{x2} while keeping their sum constant. Figure 5.5 illustrates the brake distribution influence.

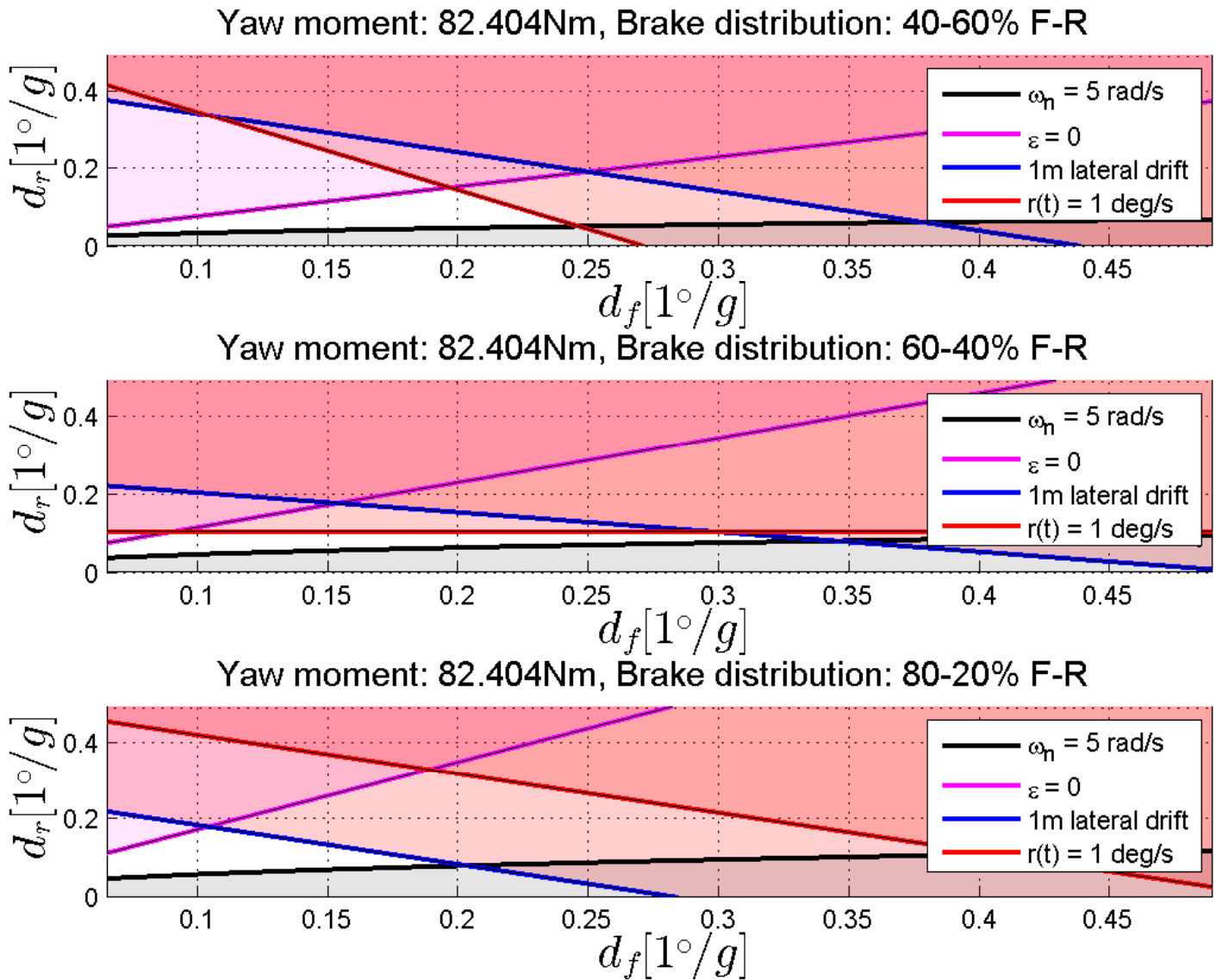


Figure 5.5: Stability limits for different brake distribution

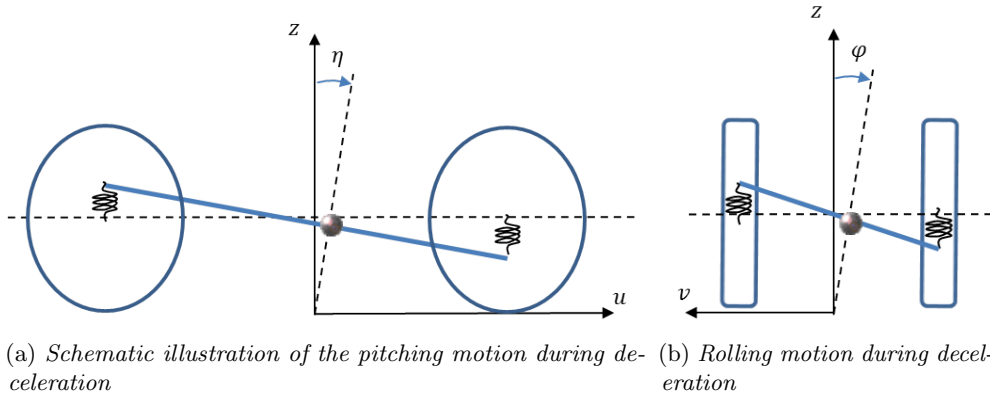
As seen in the figure, shifting the focus of the brake force will change the limits that constitutes the boundaries for the unshaded area of stable compliances. Focusing the brake force to the rear axle of the vehicle will give

characteristics closer to a oversteered vehicle which is the reason that the yaw velocity acts as a governing limit for the stable region. Focusing the brake force to the front axle of the vehicle will the opposite vehicle characteristics, more of an understeered vehicle. Therefore, as seen in the figure, the lateral drift acts as one of the governing limits for stability.

5.3 Effects of additional model refinements

So far the model simulated does not take into account any of the model refinements or additional effects mentioned in Section 2.1, such as combined slip, aerodynamic lift force, load transfer due to pitch and roll, etc. The effect of these additions to the four wheel vehicle model is now investigated further.

To take the longitudinal load transfer due to the pitching motion into account, the quasi-static methodology described in Section 2.1.5 is used. This way a constant longitudinal deceleration force is assumed to cause a constant pitching angle of the vehicle which gives rise to a constant load transfer for the tyre normal forces. The pitching motion of the vehicle is illustrated in Figure 5.6a.



Using the simplification that η is constant during the deceleration a constant normal force factor is added and subtracted to the front and rear wheel's normal forces respectively. This quasi static longitudinal load transfer is quantified by the following expression [15]:

$$\Delta F_{z,pitch} = \frac{h}{\ell} F_{x,tot} \quad (5.16)$$

Load transfer from the right hand side to the left hand side, or vice versa, will occur due to the rolling motion of the vehicle, i.e. motion in the φ -degree of freedom illustrated in Figure 5.6b. Just as for the longitudinal load transfer a quasi-static approach is used to obtain the lateral load transfer. Assuming that the vehicle travels along a circular path, i.e. steady state cornering, and that the vehicle is rigid, the lateral load transfer from the inner to the outer wheels becomes [15]:

$$\begin{cases} \Delta F_{z,roll} = \sigma m a_y \\ \sigma = \frac{h}{4w} \frac{(2(k_{1\varphi} + k_{2\varphi}) - mgh)}{(k_{1\varphi} + k_{2\varphi} - mgh)} \end{cases} \quad (5.17)$$

where $k_{i\varphi}$ is the torsional stiffness for the i :th wheel axle, computed as shown below [11]:

$$k_{i\varphi} = (k_{iR} + k_{iL}) \frac{w^2}{2} \quad (5.18)$$

Combining the effects roll- and pitch motion with the aerodynamic lift force, Equation 2.8, gives complete expression for the tyre normal forces shown in Equation 5.19, which is both time dependent and dependent on the applied brake force.

$$F_{z1R} = F_{z1,static} + \Delta F_{z,pitch}(F_x) + \Delta F_{z,roll}(t) + \Delta F_{z1,lift}(t) \quad (5.19a)$$

$$F_{z1L} = F_{z1,static} + \Delta F_{z,pitch}(F_x) - \Delta F_{z,roll}(t) + \Delta F_{z1,lift}(t) \quad (5.19b)$$

$$F_{z2R} = F_{z2,static} - \Delta F_{z,pitch}(F_x) + \Delta F_{z,roll}(t) + \Delta F_{z2,lift}(t) \quad (5.19c)$$

$$F_{z2L} = F_{z2,static} - \Delta F_{z,pitch}(F_x) - \Delta F_{z,roll}(t) + \Delta F_{z2,lift}(t) \quad (5.19d)$$

Using the lateral force dependent tyre models shown in Equations 2.3 and 2.4 the dynamic effects of pitch- and roll motion and the aerodynamic effects are now included in the model.

The impact of adding load transfer dependence, lift force, and combined slip are now analysed by including these effects in the four wheel model derived in Section 3.1. The effects are shown in the figures below in the manner of yaw velocity, lateral acceleration and lateral drift for two different braking procedures.

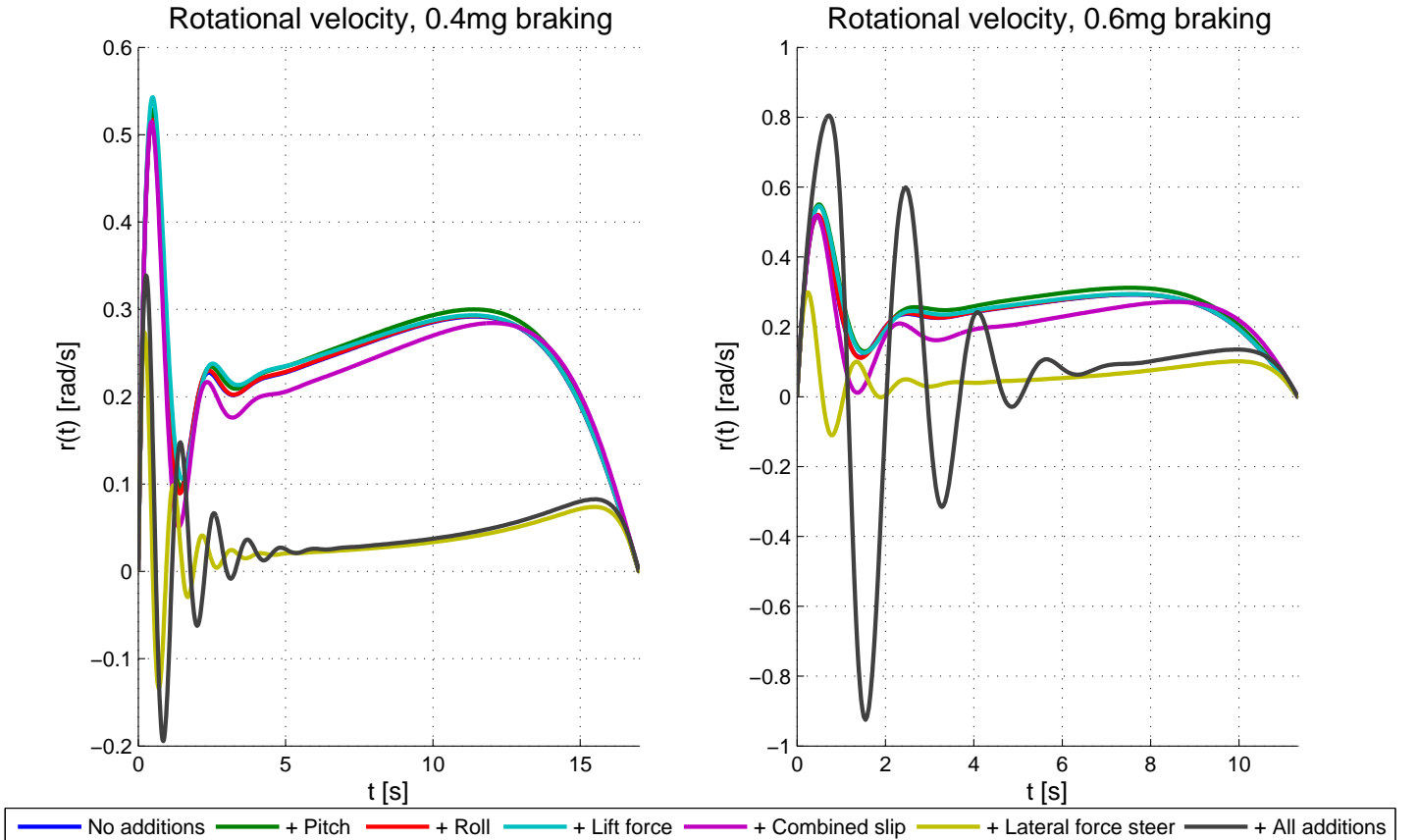


Figure 5.7: Rotational velocity for different effects added to the model

Studying the figure showing the yaw velocity with a brake force of $0.4mg$ (the left figure), it can be seen that the effect influencing the result the most is the lateral force steer and is similar to the curve with all effects taken into account. Analysing the figure illustrating the yaw velocity with a brake force of $0.6mg$ it is clearly seen that studying a model only which only includes the lateral force steer will not be sufficient. Including all of the effects for the case of $0.6mg$ (the right figure) brake force the result does not resemble any of the other effects taken into account on their own. This clearly show the nonlinearity of the system, and therefore using the superposition principle and summarizing the impact of each dynamic effect will not give the same result as if the simulation is carried out with all the effects taken into account at simultaneously.

However, the immense impact of including the lateral force steer effect is thought to be unrealistic. This as the model for the steer angle change due to lateral and longitudinal forces requires that the fluctuations are small, as mentioned in Section 2.1.3. As the rotational velocity is the governing parameter in the analysis large oscillations cannot be allowed for the steer angle model used to be valid.

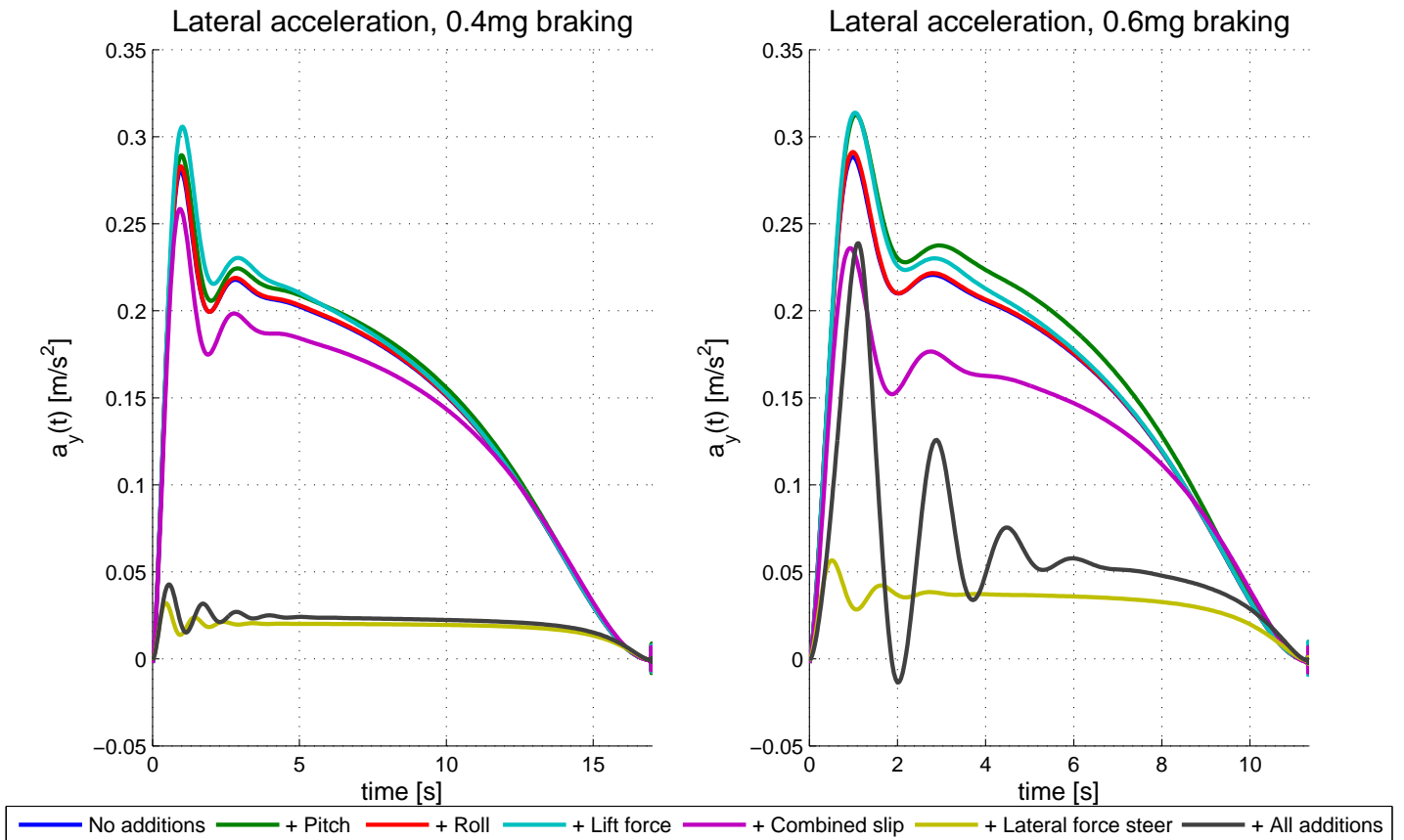


Figure 5.8: *Lateral acceleration for different effects added to the model*

Studying the Figure 5.8 illustrating the lateral acceleration, the same behaviour as for the yaw velocity is seen for both brake force scenarios. That the lateral force steer effect captures the behaviour of the complete model very well in the case of lower brake force but is not nearly sufficient for the case of harder brake force, where all effects must be included. However, the figure clearly shows that the lateral acceleration is neither small nor constant, which again gives reason to question the validity of the lateral force steer model.

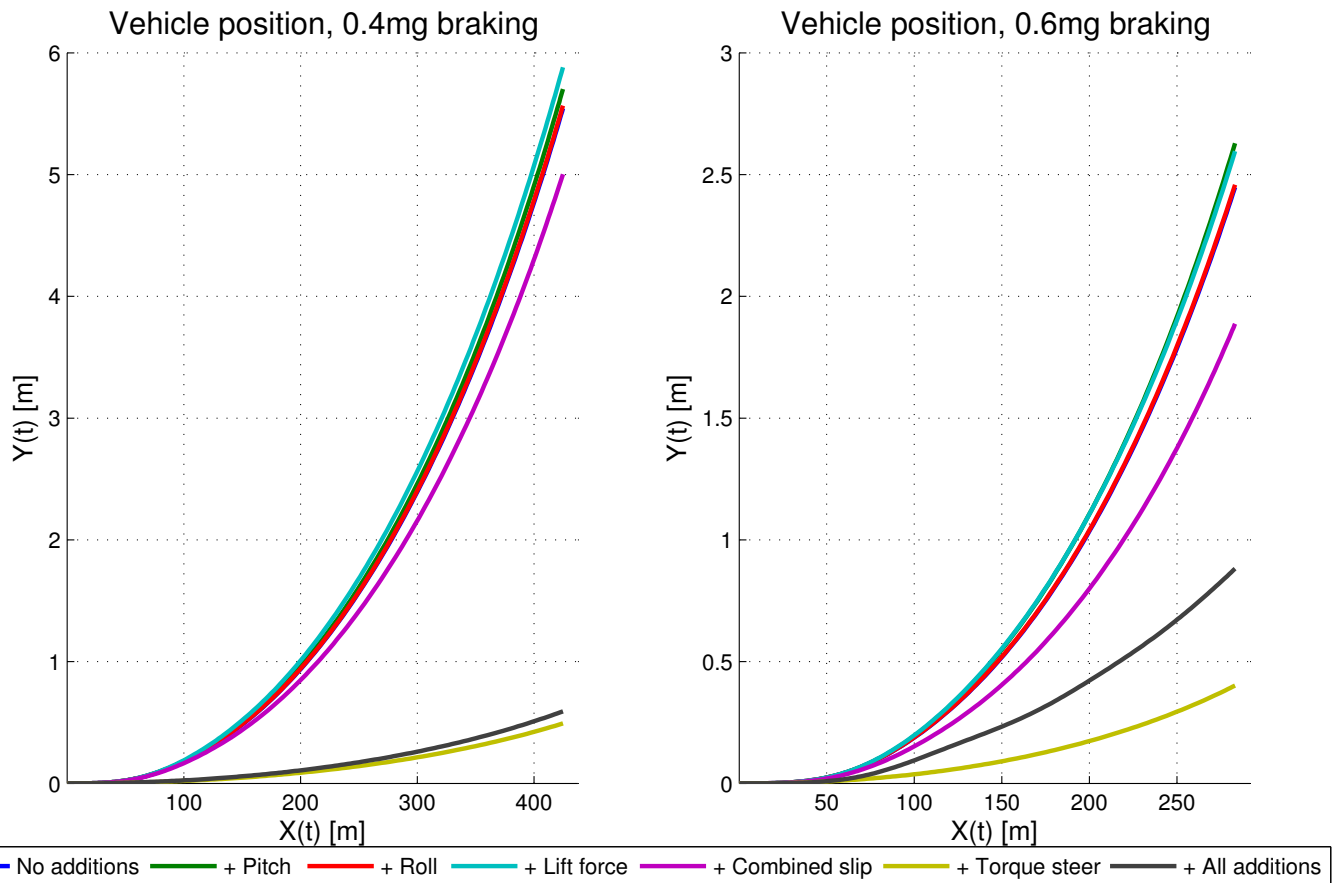


Figure 5.9: Lateral drift during braking procedure for different effects added to the model

As seen in the Figure 5.9, the impact of each added effect is very similar for all studied parameters, for instance the addition of load transfer effects due to pitch and roll show little impact on the lateral drift outcome, whereas the lateral force steer effect has a great influence on the outcome. From the result of the parameters studied the nonlinearity of the system clearly shows as the impact of adding all effects to the model at once is far from what would have been obtained if the impact of including each effect individually would have been added together.

Important to notice is the effect the brake force has on the stability of the vehicle, especially when combining all additional effects. For harder braking the vehicle experiences more pitching motion and thus the load transfer from the rear axle to the front axle is larger which gives rise to wobbling- and shimmy-like behaviour as the normal forces of the rear wheels decrease, i.e. giving the vehicle somewhat more oversteered characteristics. The impact of taking the combined slip into account is much stronger for the case of harder brake force as the longitudinal brake force in this case consumes more of the tyre's total grip than in the more moderate braking.

Judging only by the appearance of the curves for the lateral drift shown in Figure 5.9, the braking procedure could be assumed as quasi static cornering. However, Figures 5.7 and 5.8 clearly shows that this assumption cannot be considered reasonable due to the strong oscillations.

6 Discussion

The following chapter highlights the results and academic findings of the thesis work and puts the obtained results in relation to previous research within the area. The influence of assumptions and limitations of the study is also discussed as well as recommendations for future courses of action.

6.1 Compilation of obtained results

The two main result outputs of the thesis are the analytical two wheel model and the analysis of different effects and stability limits. The major findings of the first and perhaps most significant output, the analytical model, are that the possibilities for deriving analytical vehicle models does not stop where Koiter and Pacejka finishes their derivation of an analytical model in the article *Skidding of vehicles due to locked wheels*[2], i.e. the analytical vehicle model can be derived much further. However, another finding of significance in the analytical study which almost is in contradiction to that just mentioned is that the requirement of analytical solvability acts as bottleneck of great proportions when it comes to including advanced effects and phenomena in the model.

The analysis of the impact of different effects in the vehicle model shows that there are several effects with great influence of the vehicle's high speed stability. Although only a handful of effects is analysed in this thesis, the conclusion can still be drawn that additional vehicle dynamical effects of this kind are of great importance as their effect on the outcome in the stability analysis cannot be neglected. A clear example of this is shown in the study of the lateral drift which shows that without any additional effects in the four wheel model the vehicle drifts several meters of the road even though the disturbance of the model is very small. It is therefore important to include more effects of significance in the analytical model for it to be more reliable and for it to capture more phenomena of interest in stability analysis. The nonlinearity in the outcome when combining several additional effects in the simulation is an important finding in the second part of the thesis output. The conclusion of this is that for improving the analytical model, the model must be able to include several of the vehicle dynamical effects studied here simultaneously, i.e. the outcome of each individual model improvement cannot be added using the superposition principle to obtain the final outcome. The study also shows that the majority of the additional effects studied cannot be added to the model retrospectively as they often are highly reliant of time dependent parameters and therefore effect and alter the procedure used when deriving the governing differential equation for the yaw velocity.

The frequency analysis chapter clearly shows the need for inherent vehicle stability as the values of both the gain in lateral acceleration and the yaw velocity are in dangerous regions at high speeds, but improves significantly as the velocity of the vehicle is decreased. This need for inherent vehicle stability is also somewhat confirmed by the stability analysis as the front and rear compliance of the vehicle are truly governing in determining if whether or not a vehicle is stable. This analysis is fairly brief in the thesis and could, or most likely should, be done more thorough to get the most out of the analytical two wheel model derived in the first half of the thesis.

In addressing the question regarding similarities and differences between expected results and actual results the focus falls on the derivation of the analytical model. Obtaining analytical solvability without allowing a great deal of inaccuracy when deriving the analytical model is a bottleneck more restricting than first expected. In the thesis the limit for analytical solvability is set by the software Wolfram Mathematica combined with various reformulations and series expansions from mathematical handbooks. This limit is indeed questionable as the limit of Mathematica is not the final, definite limit of analytical solvability.

Putting the analytical model in relation to previous research within the field of analytical vehicle models the work of Professor Koiter and Professor Pacejka [2] is the most obvious reference candidate as it has been starting point of the thesis. The analytical model derived in this thesis can be seen as taking Koiter and Pacejka's model one step further. This as their approach of solving the governing differential equation of the yaw velocity using Bessel functions has been used to some extent, but expanded and developed further as it now handles more disturbances and most importantly are fully integrable. These two improvements are of great importance as far more information can be obtained from the model, which in turn gives that the model is of interest in more types of analyses. Therefore, to comment on the thesis' possible contribution to the research

within the field of analytical vehicle models, it shows that the model presented by Koiter and Pacejka is *not* the final stage of analytical vehicle models. The analytical model derived in this thesis are more general and more usable, but still very far from the final stages in the research of analytical vehicle model research.

6.2 Influence of assumptions and limitations

The influence of the limitations stated in the introduction of the thesis cannot be overlooked as they to a large extent are crude simplifications of the real case of a vehicle braking at high speed. Limitations such as:

- No driver steer angle input, i.e. the driver does not rotate the steering wheel
- Suspension and tyre characteristics assumed constant
- Pitch and roll axes located in ground plane
- Rigid vehicle body
- Flat road surface
- No rotating wheels

are all crude simplifications of real vehicle and real operating conditions whose influence of the thesis outcome must be discussed. What the outcome would be if these limiting simplifications would be excluded and the complete physical behavior of these effects would to be included in the analysis is very hard to predict without a great deal of experience within the field. In the real life situation of hard braking at high speed the driver steer angle input could possibly be to the worse in terms of the vehicle being stable. Whereas including the complete effects of the suspension and chassis would most likely improve the stability of the model. The lack of test data makes it extremely difficult to determine the actual influence these limitations have in the outcome of the thesis.

When analysing the four wheel model and especially when deriving the analytical two wheel model several approximations are made for the system to be solvable. These approximations are worth analysing a bit further to determine if their validity might be questionable or not, some of the approximations made are:

- Small slip angles α
- Small angles in all rotational degrees of freedom; yaw, pitch, and roll
- Small lateral velocity v
- Quasi static load transfer due to pitch and roll
- Step function-like disturbances

The approximation of small angles for the rotational degrees of freedom gives that the time derivatives of these are also assumed to be small, which gives that a large number of terms are eliminated by the assumption that products of small terms are approximatively zero. As the study only considers the case of the vehicle traveling in a straight line while braking, these assumptions are to be considered valid as these angles will be small during the entire braking procedure. The impact these assumptions has on the outcome of the analyses is therefore be negligible. The same motivation holds for the lateral velocity, as it will be small compared to the longitudinal velocity for the entire braking procedure considered this study.

Assumptions that might influence the outcome more than aforesaid assumptions are the assumptions of quasi static load transfers in the numerical simulation of the four wheel model and the assumption that the disturbances are acting as step function-like disturbances. Using quasi static load transfer for the roll dependent load transfer is a crude simplification of the case analyzed. At the initial phase of the braking procedure the rotational velocity shows oscillating behaviour which would give an oscillating lateral load transfer. Using a quasi static expression the oscillating lateral load transfer is not taken into account to full extent, which might give a non-negligible impact in the lateral drift during the brake procedure. In the case of load transfer due to the pitching motion of the vehicle, quasi static assumption is more appropriate than in the lateral load transfer case.

This as the oscillations in the yaw degree of freedom does not affect the pitch degree of freedom to the same extent.

The assumption that the disturbances are step-function like, meaning that the disturbance amplitude is not ramped up to its final value, is also a crude assumption of the real situation which may have great influence of the results. This is a simplification of the real case when the brakes are being applied heavily at the initial phase of the braking procedure. If the disturbing moment arises due to uneven brake distribution, then ramping up the amplitude of the disturbance would be closer to the real case as the brake force applied by the driver acts more as a steep ramped function than a step function. Using a ramped disturbance would most likely give less oscillating behaviour in the initial phase of the braking procedure, thus giving better correlation between the analytical flat two wheel model and the four wheel numerical model.

The model for the steer angle change due to the lateral and longitudinal forces, see Equation 2.6, proved in Section 5.3 to be invalid. This as the model requires for the lateral and longitudinal accelerations to be small or moderate with constant or slightly oscillating behaviour. The longitudinal acceleration was known to be large on beforehand, therefore the assumption was made that the violation of this requirement would not have devastating effects for the outcome. However, the lateral accelerations proved to violate this requirement as well, which led to that none of the requirements needed for steer angle model to be valid were fulfilled. This result of this is that the entire usage of the lateral force steer model, both in the analytical and numerical model, is invalid.

6.3 Future recommendations

Since the thesis consists of two clearly defined outputs the recommendations for future courses of action will be separated in the same way, i.e. focused on improvements of the analytical model and on the effects of adding various effects to the model and analysing their effect on the stability.

The first and perhaps most obvious recommendation regards the most obvious flaw in the thesis, namely the lack of experimental data. For future research of same analytical nature to be able to gain any ground towards becoming an accepted model comparison with experimental data is a necessity.

The derivation of the analytical model should be preceded by an extensive analysis of different vehicle dynamical effects to see which effects the analytical model derivation should focus on including. This analysis could be done by numerical simulations or perhaps by detailed literature studies. More effects than the ones mentioned in this thesis should be studied and the ones studied in thesis should be studied more thoroughly. This will most definitely increase the accuracy of the analytical model compared to the experimental results. Effects that, judging from this study, could be included in the analytical model are adding springs and dampers to the analytical model, including pitch and roll, and using a more sophisticated tyre model.

Another recommendation regarding the software used in derivation of the analytical model is to focus the analytical calculations and latter analysis of the model to one software. As mentioned in the introduction of this thesis, the work is carried out using a combination of both Matlab's Symbolic Math Toolbox and Wolfram Mathematica which is not optimal as it introduces an unnecessary source of errors. Matlab's Symbolic Math Toolbox is improved for every new version so chances are that future versions will be equally powerful as Wolfram Mathematica when it comes to analytical calculations.

As mentioned previously the model used for the steer angle change during the braking procedure proved to be invalid for the case studied in this thesis. Therefore, future studies must use another model for this effect. The writers would recommend the following model:

$$\delta_{T_s} = -F_y \frac{\partial \delta}{\partial T_s} \left(\xi_{Tr} + \frac{F_x}{K_y} \right) \quad (6.1)$$

with both the lateral and longitudinal forces, F_y and F_x , filtered using a basic first order filter. This to get more realistic response in the tyre and vehicle dynamics as the initial transient oscillations would be reduced by the filters. For the real case the response in the tyres and in the flexibility in steering system is not instant unlike in the models presented in this thesis. In the real case all responses during the braking procedure

builds up slowly with very little initial transient oscillations. Using the model for steer angle change shown in Equation 6.1 with first order filters for the forces would capture the behaviour of the forces and the dynamic response due to the forces building up slowly and not react with full impact instantaneously.

7 Conclusion

The subject studied in this thesis are of importance, of *great* importance if velocities of the same magnitude as studied in this thesis were more common, as operating a vehicle at extreme velocities requires both major skill and experience of the driver. This is clearly shown in the frequency response analysis, where the lateral acceleration gain is of much less dramatic proportions at lower velocities. This is why the inherent stability of the vehicle is a key factor in its high speed stability. This is in turn where the analytical model derived in this thesis can be of use. Since the need for simulating the braking procedure is eliminated, the model may advantageously be used for parameter analyses to help find important, governing factors and parameters and also help show the influence of various changes of these parameters. This as the computational power needed for the analysis of an analytical model is much less than that of a model which requires numeric simulation of each parameter set. If developed further, the model could perhaps be implemented in the vehicle's active safety system. This as the model does not requires any numeric simulation or iterations.

The main outputs of thesis, the analytical model and the study of additional vehicle dynamical effects, satisfies the research question posed in the initial phase of the study. If not completely then at least to a large extent. The analytical model shows potential for further development as it could be made more compact and include more dynamical effects. Effects that the second part of the study proved to be of importance. A significant part of the thesis results regarding the general research of the subject at matter is that the maximum potential for an analytical vehicle model is not yet reached, far from it. Further development of analytical models would not be in vain as the simplicity of using an analytical model is an attractive attribute, not only in an academic sense but also from the vehicle industries point of view. This as it could help the increase expansion and understanding of vehicle stability, mainly by use of its computational efficiency in iterative parameter and behaviour studies.

The thesis shows, at least to some extent, that the research area and improvement of analytical vehicle models are far from fully explored. The analytical two wheel model, which is to be seen as the main output of the thesis, is a small step in the right direction of the research within analytical vehicle stability. However, the need of comparing the analytical model with experimental results is not to be overlooked. This comparison is trivial for verifying the quality of the analytical model and without this the result based on the analytical two wheel model cannot be trusted. This is a great flaw in the thesis which the writers of the thesis are well aware of. Viewed from a slightly critical point of view, the facts stands that without comparison with experimental results the model analyses of this thesis can merely be seen as qualified guesses of a vehicle's behaviour in a high speed braking situation.

Bibliography

- [1] Masato Abe. *Vehicle Handling Dynamics - Theory and Application*. Elsevier Ltd, Amsterdam, The Netherlands, 2009.
- [2] Hans Pacejka , Warner Koiter. Skidding of vehicles due to locked wheels. *Institution of Mechanical Engineers*, 1968.
- [3] Johan Wedlin, Lars-Runo Tillback, Olof Bane. Combining properties for driving pleasure and driving safety: A challenge or the chassis engineer. *Automobile Safety: Present and Future Technology*, 1992.
- [4] Haim Baruh. Another look at the describing equations of dynamics. Technical report, Department of Mechanical and Aerospace Engineering Rutgers University, Piscataway, New Jersey, 1 2000.
- [5] Karl Gustav Andersson, Lars-Christer Böiers. *Ordinära differentialekvationer*. Studentlitteratur, Lund, Sweden, second edition edition, 1992.
- [6] Anders Boström. *Rigid Body Dynamics Course Compendium, MMA092*. Chalmers University of Technology, Gothenburg, Sweden, 2012.
- [7] Lennart Råde, Bertil Westergren. *Mathematics Handbook for Science and Engineering*. Studnetlitteratur AB, Lund, Sweden, 2010.
- [8] Bengt Jacobson, *et al.* *Vehicle Dynamics Compendium for Course MMF062*. Chalmers University of Technology, Gothenburg, Sweden, third edition edition, 2012.
- [9] Barys Shyrokau, *et.al.* Vehicle dynamics with brake hysteresis. Institution of Mechanical Engineers. SAGE Publications, 2013.
- [10] Thomas D. Gillespie. *Fundamentals of Vehicle Dynamics*. Society of Automotive Engineers, Inc, 1992.
- [11] Matthijs Klomp. *On Drive Force Distribution and Road Vehicle Handling*. PhD thesis, Chalmers University of Thechnology, 2007.
- [12] Jack Hale, Sjoerd M. Verduyn Lunel. *Introduction to Functional Differential Equations*. Springer Verlag New York inc, 1993.
- [13] Leonard Meirovitch. *Methods of analytical dynamics*. Dover Publications, Mineola, New York, 2003.
- [14] Shinichiro Horiuchi, Kazuyuki Okada. Evaluation of vehicle maneuverability to variations in mass center location and yaw inertia using controllability region analysis. Technical report, Department of Mechanical Engineering, College of Science and Technology, Nihon University, 2012.
- [15] Hans B. Pacejka. *Tyre and vehicle dynamics*. Butterworth-Heinemann,Oxford,UK, second edition, 2006.
- [16] Rajesh Rajamani. *Vehicle Dynamics and Control*. Department of Applied Mechanics, Chalmers University of Thechnology, Gothenburh, Sweden, 2012.
- [17] Clay C. Ross. *Differential Equations: An Introduction with Mathematica*. Springer Science and Business Media Inc., New York, second edition, 2004.
- [18] Roger A. Wehage. Vehicle dynamics. *Journal of Terramechanics*, 24(4), 1987.

